Supporting Information
for

Pseudo electron-deficient organometallics: limited reactivity towards electron-donating ligands

Anaïs Pitto-Barry, Alexandru Lupan, Markus Zegke,Thomas Swift, Amr A. A. Attia, Rianne M. Lord, and Nicolas P. E. Barry

Contents

1. Materials and Methods 3
Materials 3
Instrumentation 3
Methods 4
2. Synthesis and characterisation of complexes 1 – 4 4
Synthesis of ([(η^6-*p*-cymene)Ru(benzene-1,2-dithiolato)] (**1**) 4
Synthesis of [(η^6-*p*-cymene)Os(benzene-1,2-dithiolato)] (**2**) 4
Figure S1. ^{13}C NMR spectra of complexes **1 – 4** ($CDCl_3$, 100 MHz, 298 K). 7
Figure S2. FTIR spectra of complexes **1 – 4**, recorded as powders (spectra have been shifted along the y axis for clarity). 8
Figure S3. Mass spectra of complexes **1** and **2** in methanol solutions, recorded in ESI+ mode. 9
Figure S4. Solid state structures of **1** and **3** with thermal ellipsoids at 50% probability level. The hydrogen atoms are omitted for clarity. 10
3. Titration of complexes 1 – 4 with pyridine 11

Figure S5. UV-Vis spectra of the titrations of complexes **1 – 4** with pyridine in CH_2Cl_2 (10^{-4} M, 298 K). 11

4. Synthesis and characterization of complexes 5 – 8 12

Synthesis of [(η^6-*p*-cymene)Ru(3,6-dichlorobenzene-1,2-dithiolato)] (**5**) 12

Synthesis of [(η^6-*p*-cymene)Os(3,6-dichlorobenzene-1,2-dithiolato)] (**6**) 12

Synthesis of [(η^5-pentamethylcyclopentadiene)Rh(3,6-dichlorobenzene-1,2-dithiolato)] (**7**) 12

Synthesis of [(η^5-pentamethylcyclopentadiene)Ir(3,6-dichlorobenzene-1,2-dithiolato)] (**8**) 13

Figure S6a. ^{13}C NMR spectra of complexes **5** and **6** ($CDCl_3$, 100 MHz, 298 K). 14

Figure S6b. ^{13}C NMR spectra of complexes **7** and **8** ($CDCl_3$, 100 MHz, 298 K). 15

Figure S7. Infra-red spectra of complexes **5 – 8**, recorded as powders (spectra have been shifted along the y axis for clarity). 16

Figure S8a. Mass spectra of complexes **5** and **6** in methanol solutions, recorded in ESI+ mode. 17

Figure S8b. Mass spectra of complexes **7** and **8** in methanol solutions, recorded in ESI+ mode. 18

5. Titration of complexes 5-8 19

Figure S9. UV-Vis spectra of the titration of complexes **5 – 8** by DMAP, triphenylphosphine, and pyridine in CH_2Cl_2 (10^{-4} M, 298 K). 19

6. Crystallographic data 20

Table S1**.** X-ray crystallographic data for complexes **1**, **3**, **6**, and **8**, with s.u.s shown in parenthesis. 20

Table S2**.** Selected bond lengths (Å) for complexes **1**, **3**, **6**, and **8**. 20

Table S3**.** Selected bond angles (°) for complexes **1**, **3**, **6**, and **8**. 21

Figure S10. Packing diagram showing the short contacts of complex **1**, **3**, **6** and **8**. 21

7. Calculations data 22

Table S4**.** Distance table for the optimized structure of complex **1** (M11L/def2tzvp). 22

Table S5**.** Distance table for the optimized structure of complex **2** (M11L/def2tzvp). 23

Table S6**.** Distance table for the optimized structure of complex **3** (M11L/def2tzvp). 24

Table S7**.** Distance table for the optimized structure of complex **4** (M11L/def2tzvp). 25

Table S8**.** Molecular orbitals involved in the five main calculated singlet electronic transitions of the UV-visible spectrum of complex **1** and their relative weights determined by TD-DFT calculations. The molecular orbitals are shown in Figure 8. 25

Table S9**.** Molecular orbitals, with ranking order and energy (in a.u.) for compound **1.** 26

Table S10**.** Thermochemistry of the reactions between complexes **1 – 4**, pyridine, DMAP, and triphenylphosphine, with computed zero point corrected Gibbs free energies of all the species**.** 27

8. ^{1}H DOSY NMR 28

Figure S11. Snapshot of raw ^{1}H DOSY data from complex **1** processed using Bruker Topspin software carried out at 298 (A), 278 (B) and 328 (C) K. 28

Figure S12. Isolated ^{1}H proton signal from dimer (blue) and monomer (red) signals 29

Table S11. ^{1}H DOSY NMR of complex **1** at different temperatures. 29

9. References.....29

1. Materials and Methods

Materials

Metals chloride hydrates were purchased from Precious Metals Online.

All other reagents were obtained from commercial suppliers and used as received. THF was distilled over calcium hydride. Procedures were performed under nitrogen atmosphere and dried glassware, unless otherwise stated.

The $[(\eta^6\text{-}p\text{-cymene})MCl(\mu\text{-}Cl)]_2$ (M: Ru and Os) and $[(\eta^5\text{-}C_5(CH_3)_5)MCl(\mu\text{-}Cl)]_2$, dimers (M: Rh and Ir) were prepared according to literature procedures.[1] $[(\eta^5\text{-}C_5(CH_3)_5)Rh(S_2C_6H_4)]$ and $[(\eta^5\text{-}C_5(CH_3)_5)Ir(S_2C_6H_4)]$ were prepared according to literature procedures.[2]

Instrumentation

All NMR spectra were recorded on a 400 MHz Bruker Spectrospin spectrometer using deuterated solvents. Chemical shifts are reported as δ in parts per million using the residual protonated solvent as internal standard.[3] The following abbreviations are used to describe signals multiplicities: doublet (d), doublet of doublet (dd), triplet (t), quartet (q), septet (sept), multiplet (m). Diffusion-Ordered Spectroscopy was carried out using a modified Bruker Pulse sequence. Calibration of the gradient field strength was performed using a sample of H_2O in D_2O (1% v/v) doped with $GdCl_3$ (0.1 mg) as a paramagnetic relaxation agent. Gradient strengths were calibrated to provide a diffusion coefficient of 1.91×10^{-9} m^{-2} s^{-1} at 298.15 K (gradients operated from 95% to 5% using 16 points with a quadratic decay). A bipolar LED sequence as for the sample measurements was used, with sine shaped gradient pulses and gradient strengths incremented between 0.28 and 5.19 G mm-1 in 16 steps equally spaced in gradient squared. 1H diffusion measurements were recorded using an LED sequence with bipolar gradients, with sine shaped gradient strength incremented between 0.28 and 5.19 G mm^{-1} with gradient steps equally spaced linearly. Data analyses were performed using TopSpin software version 3.5 (patch level 5). Temperature accuracy for the ^1H DOSY experiments performed was ensured by initial calibration of the sample temperature to displayed sample control temperature by measurement of the shift between the residual CH_3 and OH resonances of methanol (99.8% MeOD). Diffusion distributions were calculated using the Stokes Einstein equation as previously described.[4]

Atmospheric solids analysis probe mass spectroscopy (ASAP-MS) experiments were performed on a Micromass ZMD mass spectrometer. Mass analysis was performed in positive ionisation mode. Settings are the following: source temperature 400 °C, sampling cone 14 V, corona 3.94 kV.

UV-vis spectroscopy was carried out on a Perkin Elmer Lambda 35 UV/vis spectrometer or an Agilent Cary 60 UV-vis spectrophotometer. Quartz cells with two polished sides were used.

Infrared spectra of compounds were obtained using a Perkin Elmer 100 FT-IR instrument fitted with DTGS (deuterated triglycine sulphate) detector.

XRD studies: A suitable single crystal was selected and immersed in an inert oil and mounted on a nylon loop attached to a goniometer head. The crystal data was obtained on a Bruker Apex-II CCD diffractometer using Cu-K_a radiation (l = 1.5418 Å) with 1.0° f-rotation frames. The crystal was cooled to 100 K by an Oxford Cryostream low temperature device,[5] and the full data set refinement and reduction was carried out using Saint v8.34A program.[6] Structure solution by direct methods was achieved using Olex2-1.2[7] through the use of SHELXS,[8] and the structural model refined by full

matrix least squares on F^2 using SHELXT and SHELXL.[9] Molecular graphics were plotted using Mercury program.[10] Unless otherwise stated, hydrogen atoms were placed using idealised geometric positions (with free rotation for methyl groups), allowed to move in a "riding model" along with the atoms to which they were attached, and refined isotropically.

Methods

Geometry optimizations were carried out using the M11-L DFT functional[11] coupled with the SDD basis set[12] for the metal ions and the def2-TZVP basis set[13] for the lighter elements. Vibrational frequencies were calculated to ensure the absence of imaginary frequencies and to obtain the IR spectra. UV-vis spectra were computed using the time dependent density functional theory (TD-DFT) method on the optimized structures using the same DFT functionals and basis sets. All calculations were performed in vacuum.[14] All calculations were performed by utilizing the Gaussian 09 software package.[15]

2. Synthesis and characterisation of complexes 1 – 4

Synthesis of ([(η^6-*p*-cymene)Ru(benzene-1,2-dithiolato)] (**1**)

The compound has already been synthesised following a different procedure.[16] A solution of 1,2-benzenedithiol (58 µL, 0.51 mmol, 1 eq.) and sodium methoxide (55 mg, 1.01 mmol, 2 eq.) in dried THF (15 mL) was stirred under nitrogen for one hour, an orange colour appeared after 10 min. The [(η^6-*p*-cymene)RuCl(µ-Cl)]$_2$ dimer (200 mg, 0.33 mmol, 0.5 eq.) was then added, the solution became red and was stirred for 15 min. The solvent was removed and the remaining solid was purified by chromatographic column (hexane/CH_2Cl_2 2:1). A dark yellow powder was obtained (47.3 mg, 20%)

Both the mononuclear and dinuclear complexes exist in solution, as confirmed by ^{1}H NMR and as previously reported.

^{1}H NMR (400 MHz, $CDCl_3$): 8.03 (m, 2H, $H_{arom\ benzene\ monomer}$), 7.59 (d, $^3J_{H-H}$ = 7.6 Hz, 1H, $H_{arom\ benzene\ dimer}$), 7.19 (d, $^3J_{H-H}$ = 7.6 Hz, 1H, $H_{arom\ benzene\ dimer}$), 7.13 (m, 2H, $H_{arom\ benzene}$), 6.90 (t, $^3J_{H-H}$ = 7.2 Hz, 1H, $H_{arom\ benzene\ dimer}$), 6.73 (t, $^3J_{H-H}$ = 7.0 Hz, 1H, $H_{arom\ benzene\ dimer}$), 5.70 (dd, $^3J_{H-H}$ = 8.7, 6.1 Hz, 4H, $H_{arom\ p\text{-}cymene\ monomer}$), 4.84 (d, $^3J_{H-H}$ = 6.0 Hz, 1H, $H_{arom\ p\text{-}cymene\ dimer}$), 4.45 (d, $^3J_{H-H}$ = 5.8 Hz, 1H, $H_{arom\ p\text{-}cymene\ dimer}$), 4.37 (d, $^3J_{H-H}$ = 6.0 Hz, 1H, $H_{arom\ p\text{-}cymene\ dimer}$), 4.24 (d, $^3J_{H-H}$ = 5.8 Hz, 1H, $H_{arom\ p\text{-}cymene\ dimer}$), 2.88 (sept, $^3J_{H-H}$ = 6.9 Hz, 1H, $CH(CH_3)_{2\ dimer}$), 2.71 ((sept, $^3J_{H-H}$ = 6.9 Hz, 1H, $CH(CH_3)_{2\ monomer}$), 2.35 (s, 3H, $CH_3C_{arom\ monomer}$), 2.19 (s, 3H, $CH_3C_{arom\ dimer}$), 1.34 (d, $^3J_{H-H}$ = 6.9 Hz, 6H, $CH(CH_3)_{2\ monomer}$), 1.20 (d, $^3J_{H-H}$ = 6.8 Hz, 3H, $CH(CH_3)_{2\ dimer}$), 1.17 (d, $^3J_{H-H}$ = 6.3 Hz, 3H, $CH(CH_3)_{2\ dimer}$). ^{13}C NMR (100 MHz, $CDCl_3$): 157.0, 156.1, 148.2, 130.0, 129.3, 128.9, 125.6, 122.4, 120.0, 106.4, 105.0, 100.7, 94.1, 88.7, 88.4, 87.7, 84.7, 80.3, 78.2, 77.4, 32.2, 31.7, 30.2, 24.3, 23.6, 22.8, 21.8, 20.8, 19.0. MS (AP^+): 376.9 $[M+H]^+$. UV-vis (CH_2Cl_2, 1.0 × 10^{-4} M): λ_{max} 258 (ε = 1.22 × 10^4 M^{-1}/cm), 298 (ε = 0.55 × 10^4 M^{-1}/cm), 439 (ε = 0.65 × 10^4 M^{-1}/cm), 571 (ε = 0.14 × 10^4 M^{-1}/cm).

Synthesis of [(η^6-*p*-cymene)Os(benzene-1,2-dithiolato)] (**2**)

The same procedure as for [(η^6-*p*-cymene)Ru(benzene-1,2-dithiolato)], the ruthenium analogue molecule, was followed using [(η^6-*p*-cymene)OsCl(µ-Cl)]$_2$ dimer (200 mg, 0.25 mmol, 0.5 eq.) A dark red powder was obtained (99 mg, 42%).

Only the mononuclear complex exists in solution, as confirmed by ^{1}H NMR.

^{1}H NMR (400 MHz, $CDCl_3$): 8.19 (dd, $^3J_{H\text{-}H}$ = 6.0, 3.3 Hz, 2H, $H_{arom\ benzene}$), 7.07 (dd, 2H, $H_{arom\ benzene}$), 6.05 (dd, $^3J_{H\text{-}H}$ = 16.6, 5.8 Hz, 4H, $H_{arom\ p\text{-}cymene}$), 2.64 (sept, $^3J_{H\text{-}H}$ = 6.9 Hz, 1H, $CH(CH_3)_2$), 2.50 (s, 3H, CH_3C_{arom}), 1.35 (d, $^3J_{H\text{-}H}$ = 6.8 Hz, 6H, $CH(CH_3)_2$). ^{13}C NMR (100 MHz, $CDCl_3$): 157.3, 129.2, 123.1, 97.4, 86.8, 73.0, 70.8, 32.7, 23.8, 21.3. MS (AP^+): 467.0 $[M+H]^+$. UV-vis (CH_2Cl_2, 1.0×10^{-4} M): λ_{max} 255 ($\varepsilon = 1.78 \times 10^4$ M^{-1}/cm), 297 ($\varepsilon = 0.88 \times 10^4$ M^{-1}/cm), 374 ($\varepsilon = 0.63 \times 10^4$ M^{-1}/cm), 487 ($\varepsilon = 0.14 \times 10^4$ M^{-1}/cm).

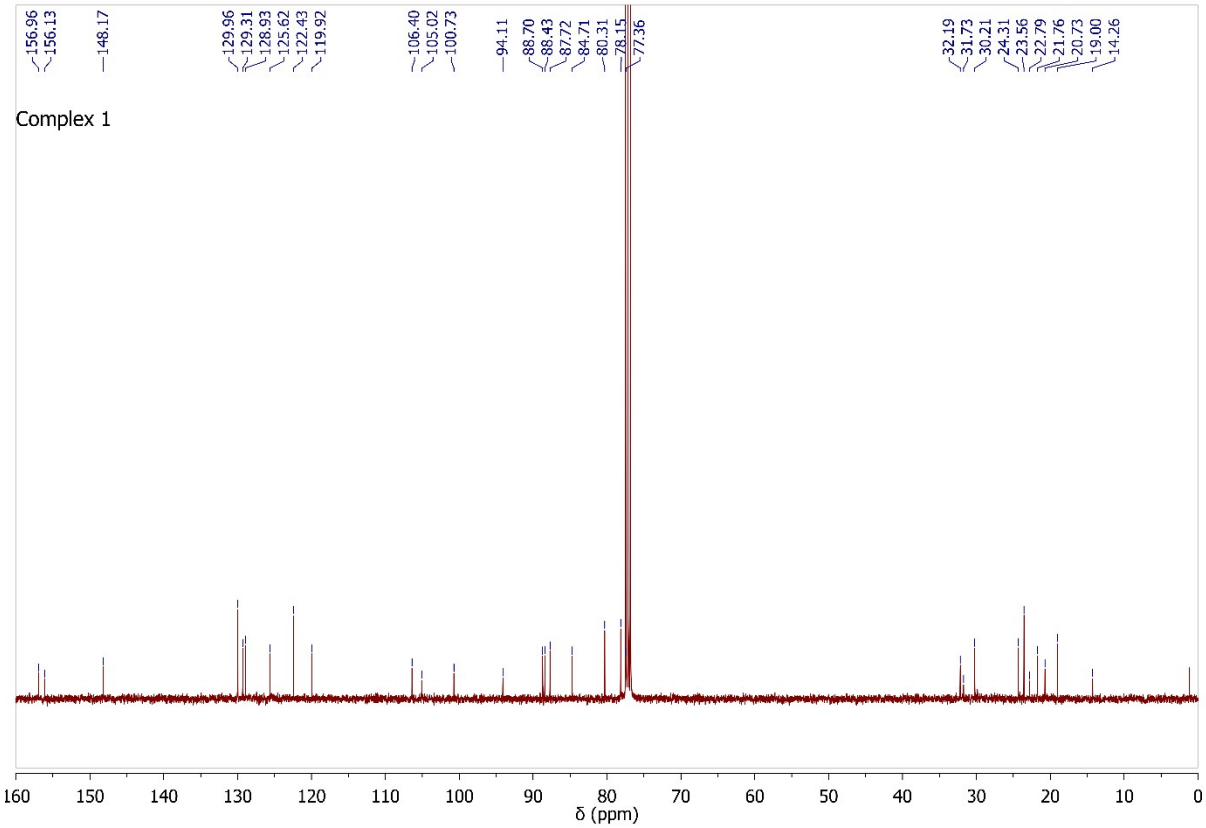

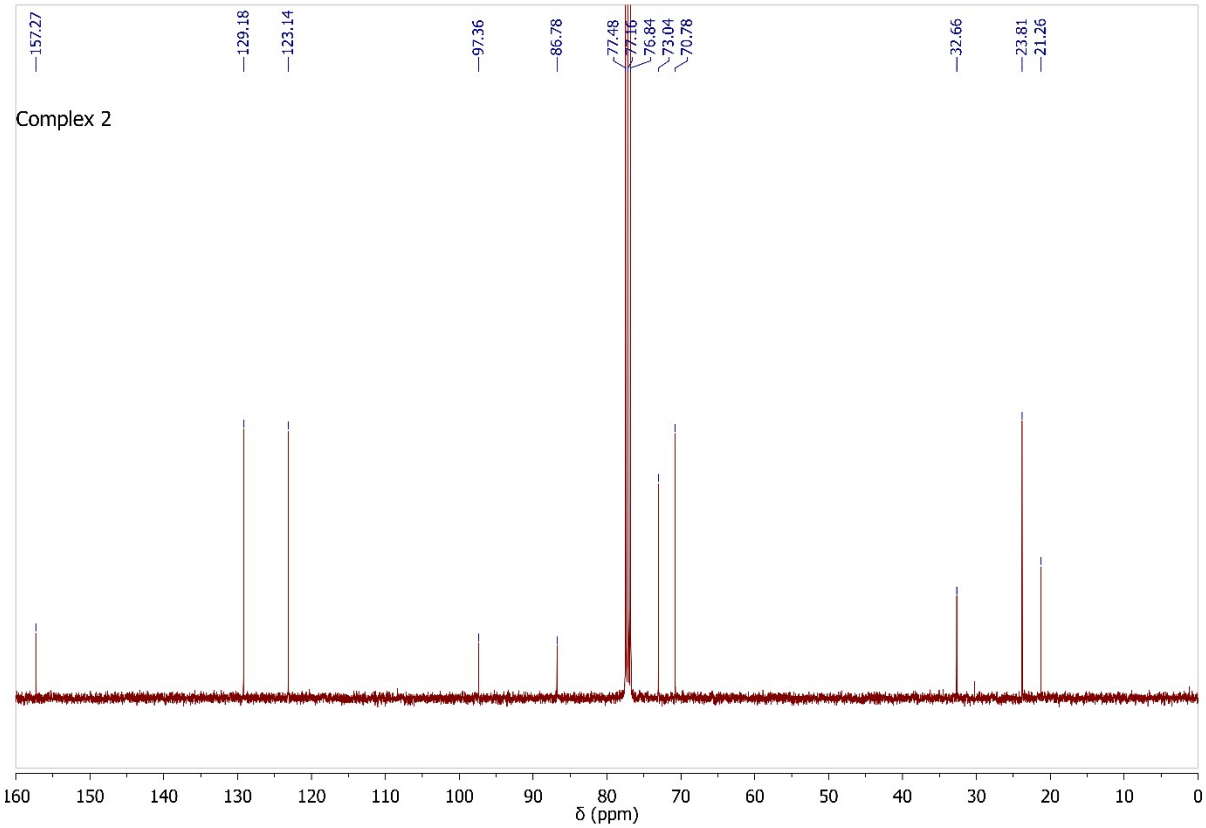
Complex 2
157.27
129.18
123.14
97.36
86.78
77.48
77.16
76.84
73.04
70.78
32.66
23.81
21.26
160
150
140
130
120
110
100
90
80
70
60
50
40
30
20
10
0
δ (ppm)

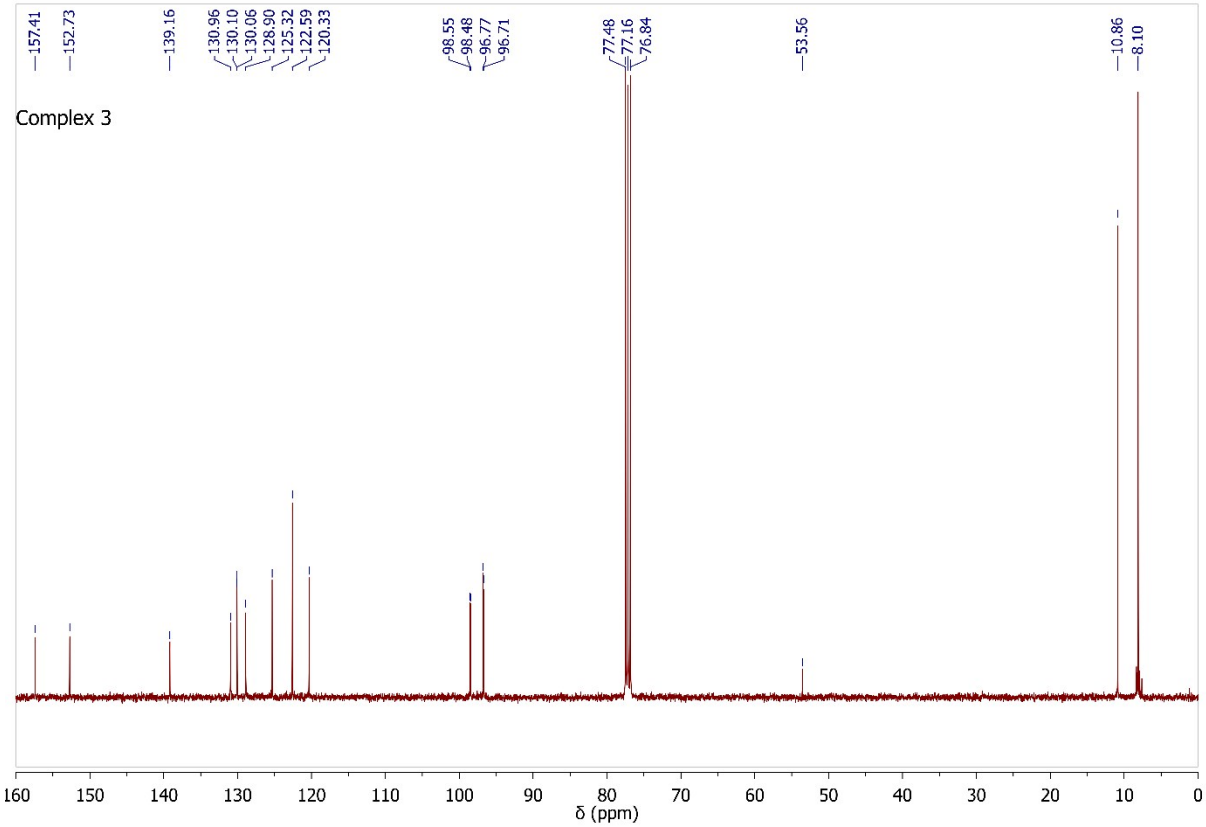

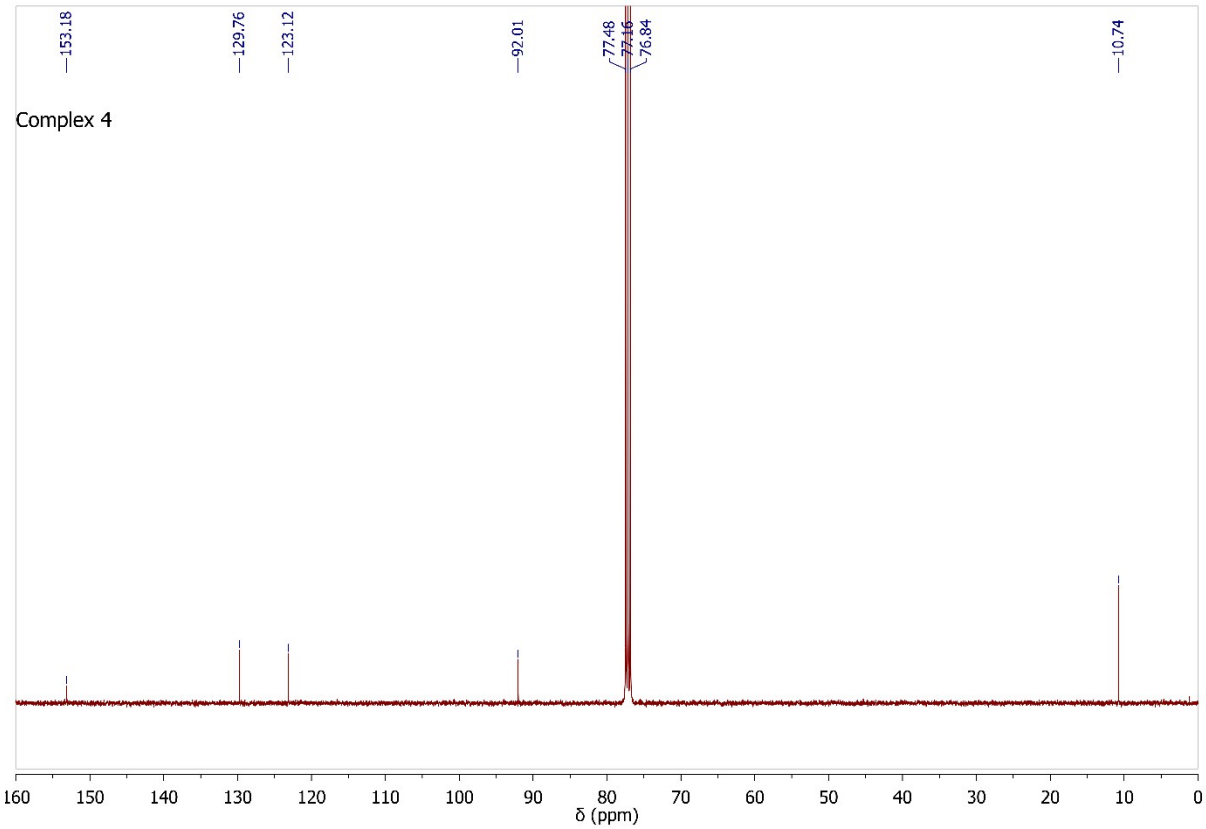

Figure S1. ^{13}C NMR spectra of complexes **1 – 4** ($CDCl_3$, 100 MHz, 298 K).

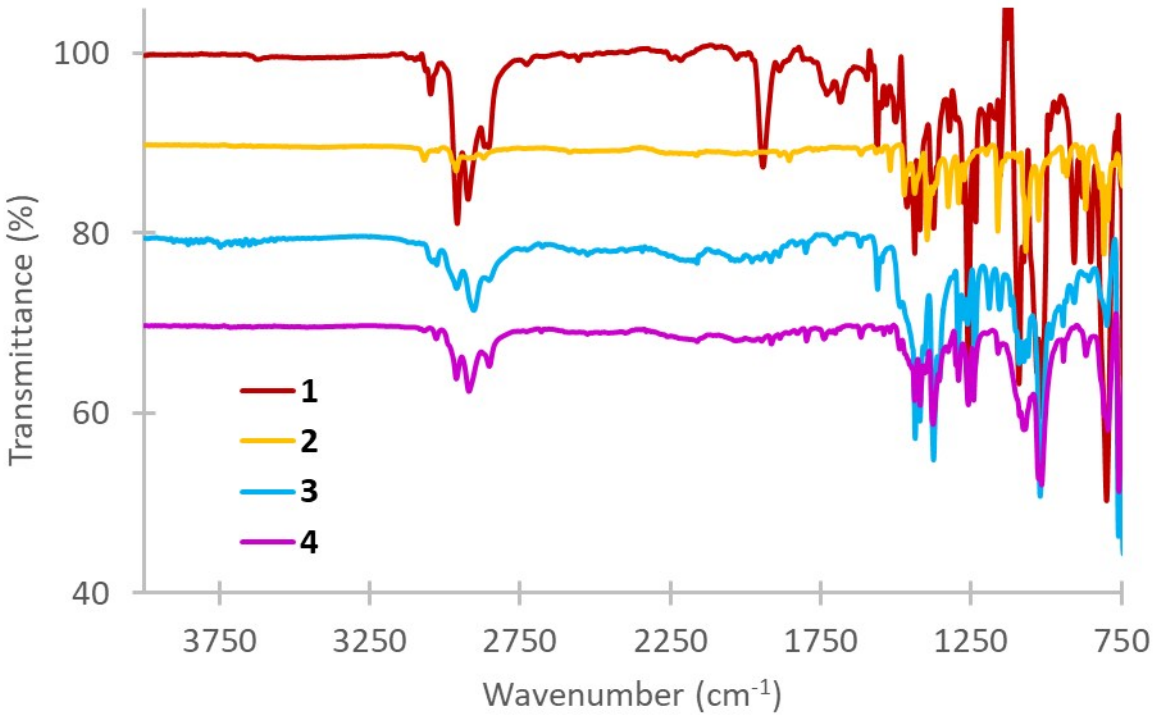

Figure S2. FTIR spectra of complexes **1 – 4**, recorded as powders (spectra have been shifted along the y axis for clarity).

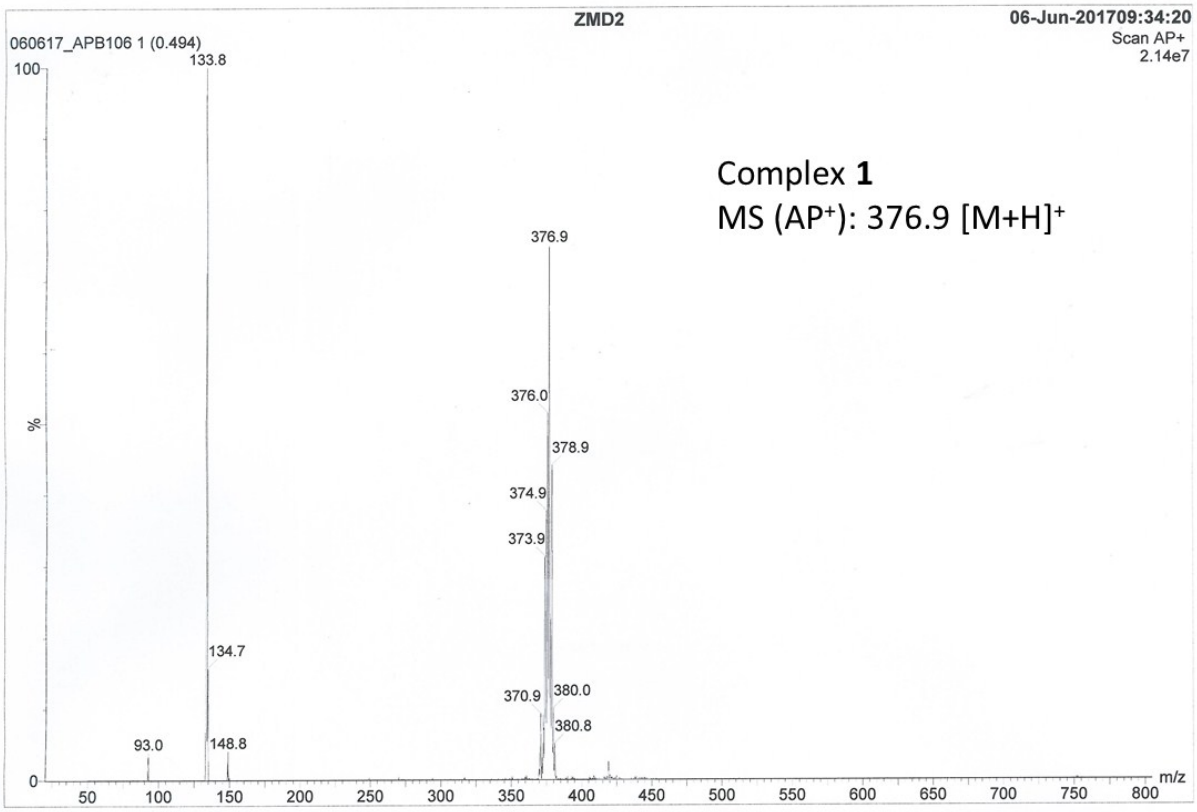

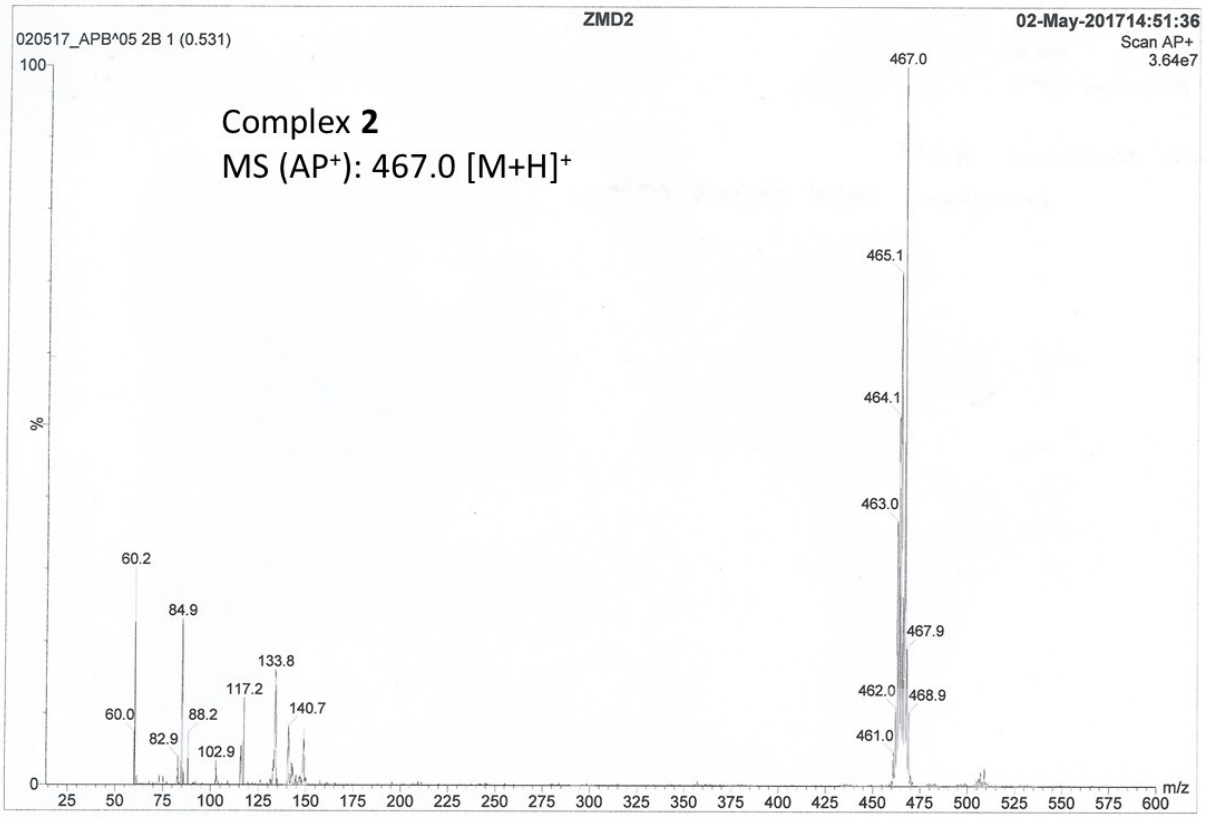

Figure S3. Mass spectra of complexes **1** and **2** in methanol solutions, recorded in ESI+ mode.

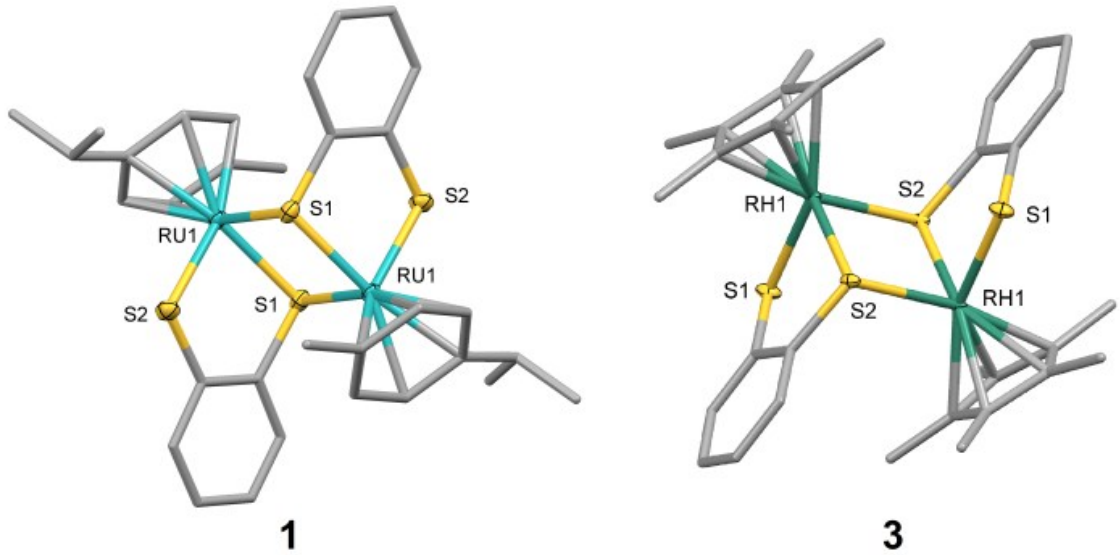

Figure S4. Solid state structures of **1** and **3** with thermal ellipsoids at 50% probability level. The hydrogen atoms are omitted for clarity.

The molecular structures for complexes **1** and **3** show a half-sandwich *pseudo*-octahedral geometry for the central metal atom. The metal atoms are capped by a *p*-cymene (**1**) or Cp* (**3**) ligand and coordinated by three S atoms, two from the benzene-1,2-dithiolato ligand, and one from an adjacent moiety, thus creating diamond-shaped $(MS)_2$ motif for these metals. The same dimeric structure of complex **1** has previously been reported;[17] however, the complex reported here crystallized in a monoclinic cell and structural solution was performed in space group $P2_1/n$. The Ru1–S bond lengths in **1** (2.378(1) and 2.377(2) Å) are close to those previously published (2.36 - 2.39 Å). The Rh1-S bond lengths in **3** (2.3589(8) and 2.3589(8) Å) are also close to literature values (2.35 – 2.40 Å).[2] Selected bond distances (Å) and angles (°): 1: Ru1-Ru1' 3.6219(5) Ru1-Cg 1.709 Ru1-S1 2.3775(13) Ru1-S2 2.3774(14) Ru1-S1' 2.4106(13) S1-Ru1-Cg 131.31 S2-Ru1-Cg 115.03 S1-Ru1-S2 84.54(5) S1-Ru1S1' 81.68(5) 2: Rh1-Rh1' 3.5189(4) Rh1-Cg 1.831 Rh1-S1 2.3589(8) Rh1-S2 2.3523(8) Rh1-S1' Rh1-S2' 2.3981(8) S1-Rh1-Cg 124.63 S2-Rh1-Cg 127.39 S1-Rh1-S2 85.05(3) S1-Rh1-S2' 84.69(3).

3. Titration of complexes 1 – 4 with pyridine

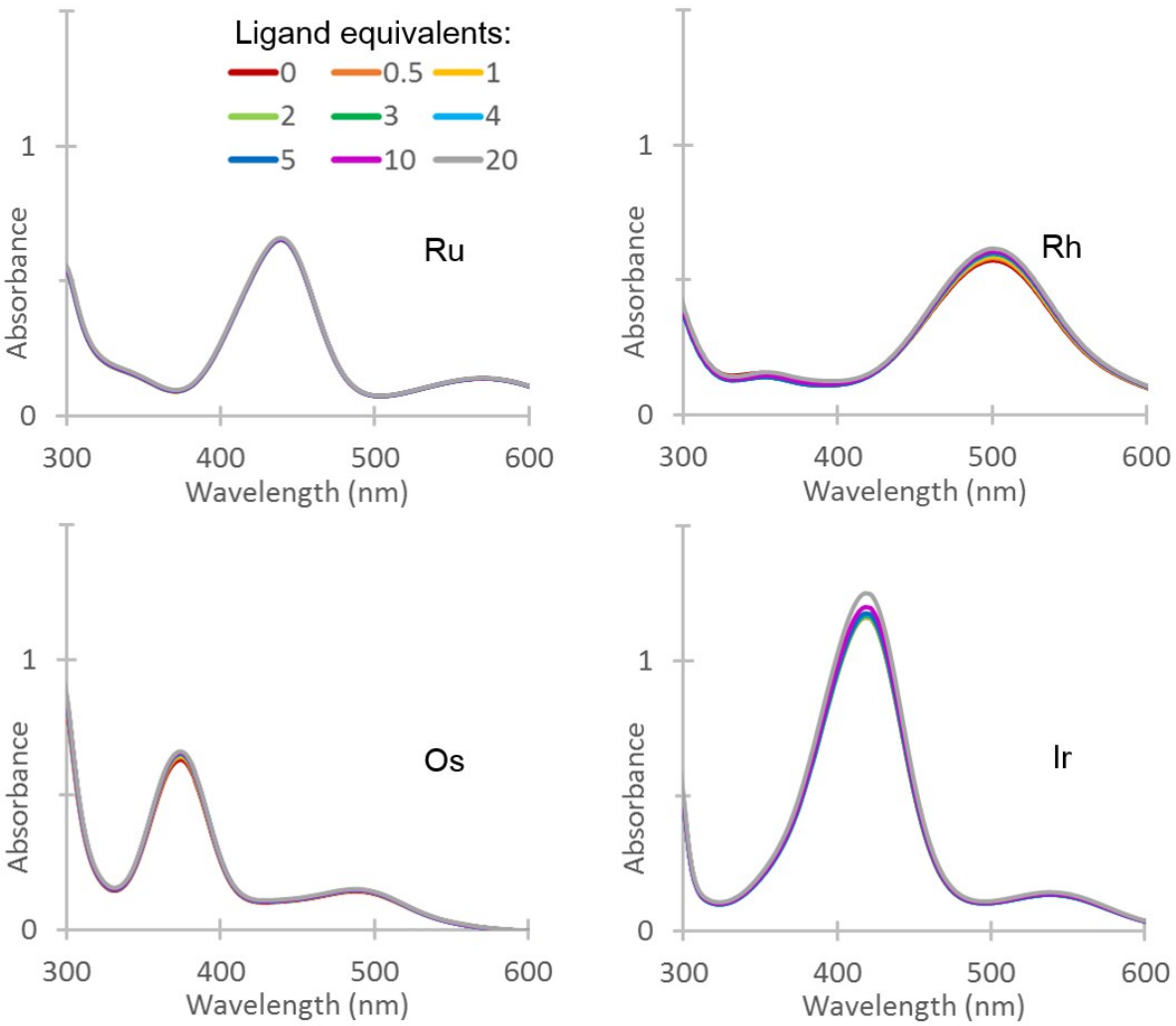

Figure S5. UV-Vis spectra of the titrations of complexes **1 – 4** with pyridine in CH_2Cl_2 (10^{-4} M, 298 K).

4. Synthesis and characterization of complexes 5 – 8

Synthesis of [(η^6-*p*-cymene)Ru(3,6-dichlorobenzene-1,2-dithiolato)] (**5**)

A solution of 3,6-dichloro-1,2-benzenedithiol (106 mg, 0.51 mmol, 1 eq.) and sodium methoxide (54 mg, 1.01 mmol, 2 eq.) in dried THF (15 mL) was stirred under nitrogen for one hour, an orange colour appeared after 10 min. The [(*p*-cymene Ru)$_2$(μ-Cl)$_2$] dimer (153 mg, 0.25 mmol, 0.5 eq.) was then added, the solution became dark red and was stirred for 15 min. The solvent was removed and the remaining solid was purified by chromatographic column (hexane/CH_2Cl_2 2:1). A red powder was obtained (58 mg, 26%).

Both the mononuclear and dinuclear complexes exist in solution, as confirmed by ^{1}H NMR.

^{1}H NMR (400 MHz, $CDCl_3$): 7.84 (d, $^3J_{H-H}$ = 6.7 Hz, 1H, $H_{arom\ benzene\ monomer}$), 7.70 (m, 1H, $H_{arom\ benzene\ dimer}$), 7.53 (m, 1H, $H_{arom\ benzene\ dimer}$), 7.27 (m, 1H, $H_{arom\ benzene}$), 7.03 (d, $^3J_{H-H}$ = 7.7 Hz, 1H, $H_{arom\ benzene\ dimer}$), 6.78 (d, $^3J_{H-H}$ = 7.7 Hz, 1H, $H_{arom\ benzene\ dimer}$), 5.82 (dd, $^3J_{H-H}$ = 9.0, 6.4 Hz, 4H, $H_{arom\ p\text{-cymene}\ monomer}$), 4.79 (d, $^3J_{H-H}$ = 6.1 Hz, 1H, $H_{arom\ p\text{-cymene}\ dimer}$), 4.66 (d, $^3J_{H-H}$ = 5.6 Hz, 1H, $H_{arom\ p\text{-cymene}\ dimer}$), 4.53 (d, $^3J_{H-H}$ = 5.6 Hz, 1H, $H_{arom\ p\text{-cymene}\ dimer}$), 4.11 (d, $^3J_{H-H}$ = 5.6 Hz, 1H, $H_{arom\ p\text{-cymene}\ dimer}$), 2.99 (sept, $^3J_{H-H}$ = 6.6 Hz, 1H, $CH(CH_3)_{2\ dimer}$), 2.62 ((sept, $^3J_{H-H}$ = 6.7 Hz, 1H, $CH(CH_3)_{2\ monomer}$), 2.31 (s, 3H, $CH_3C_{arom\ monomer}$), 2.26 (s, 3H, $CH_3C_{arom\ dimer}$), 1.26 (d, $^3J_{H-H}$ = 7.3 Hz, 6H, $CH(CH_3)_{2\ monomer}$), 1.18 (d, $^3J_{H-H}$ = 6.6 Hz, 6H, $CH(CH_3)_{2\ dimer}$). ^{13}C NMR (100 MHz, $CDCl_3$): 154.6, 131.8, 123.6, 105.4, 94.4, 81.5, 79.4, 32.1, 29.1, 23.6, 23.2, 21.7, 21.0, 14.2, 11.1. MS (AP^+): 446 $[M+H]^+$. UV-vis (CH_2Cl_2, 1.0 × 10^{-4} M): λ_{max} 260 (ε = 2.55 × 10^4 M^{-1}/cm), 306 (ε = 1.36 × 10^4 M^{-1}/cm), 426 (ε = 0.94 × 10^4 M^{-1}/cm), 564 (ε = 0.28 × 10^4 M^{-1}/cm).

Synthesis of [(η^6-*p*-cymene)Os(3,6-dichlorobenzene-1,2-dithiolato)] (**6**)

A solution of 3,6-dichloro-1,2-benzenedithiol (105 mg, 0.51 mmol, 1 eq.) and sodium methoxide (54 mg, 1.00 mmol, 2 eq.) in dried THF (15 mL) was stirred under nitrogen for one hour, an orange colour appeared after 10 min. The [(*p*-cymene Os)$_2$(μ-Cl)$_2$] dimer (191 mg, 0.25 mmol, 0.5 eq.) was then added, the solution became dark red and was stirred for 15 min. The solvent was removed and the remaining solid was purified by chromatographic column (hexane/CH_2Cl_2 2:1). A red powder was obtained (120 mg, 45%).

Only the mononuclear complex exists in solution, as confirmed by ^{1}H NMR.

^{1}H NMR (400 MHz, $CDCl_3$): 7.22 (s, 2H, $H_{arom\ benzene}$), 6.14 (dd, $^3J_{H-H}$ = 15.7, 6.1 Hz, 4H, $H_{arom\ p\text{-cymene}}$), 2.57 (sept, $^3J_{H-H}$ = 6.9 Hz, 1H, $CH(CH_3)_2$), 2.46 (s, 3H, CH_3C_{arom}), 1.31 (d, $^3J_{H-H}$ = 6.6 Hz, 6H, $CH(CH_3)_2$). ^{13}C NMR (100 MHz, $CDCl_3$): 157.2, 131.4, 124.2, 97.8, 87.2, 74.4, 72.11, 32.7, 23.9, 21.5. MS (AP^+): 534.9 $[M+H]^+$. UV-vis (CH_2Cl_2, 1.0 × 10^{-4} M): λ_{max} 260 (ε = 2.04 × 10^4 M^{-1}/cm), 304 (ε = 2.07 × 10^4 M^{-1}/cm), 368 (ε = 0.80 × 10^4 M^{-1}/cm), 488 (ε = 0.22 × 10^4 M^{-1}/cm).

Synthesis of [(η^5-pentamethylcyclopentadiene)Rh(3,6-dichlorobenzene-1,2-dithiolato)] (**7**)

A solution of 3,6-dichloro-1,2-benzenedithiol (106 mg, 0.51 mmol, 1 eq.) and sodium methoxide (54 mg, 1.00 mmol, 2 eq.) in dried THF (15 mL) was stirred under nitrogen for one hour, an orange colour appeared after 10 min. The [(pentamethylcyclopentadieneRh)$_2$(μ-Cl)$_2$] dimer (162 mg, 0.25 mmol, 0.5 eq.) was then added, the solution became brown and was stirred for 15 min. The solvent was removed and the remaining solid was purified by chromatographic column (hexane/CH_2Cl_2 3:1). A brown powder was obtained (22 mg, 10%).

Only the mononuclear complex exists in solution, as confirmed by ^{1}H NMR.

^{1}H NMR (400 MHz, $CDCl_3$): 7.24 (s, 2H, $H_{arom\ benzene}$), 1.97 (s, 15H, CH_3C_{arom}). ^{13}C NMR (100 MHz, $CDCl_3$): 151.3, 131.6, 123.8, 99.6, 10.9. MS (AP^+): 446.8 $[M+H]^+$. UV-vis (CH_2Cl_2, 1.0×10^{-4} M): λ_{max} 261 ($\varepsilon = 3.84 \times 10^4$ M^{-1}/cm), 298 ($\varepsilon = 0.66 \times 10^4$ M^{-1}/cm), 352 ($\varepsilon = 0.09 \times 10^4$ M^{-1}/cm), 479 ($\varepsilon = 0.90 \times 10^4$ M^{-1}/cm).

Synthesis of [(η^5-pentamethylcyclopentadiene)Ir(3,6-dichlorobenzene-1,2-dithiolato)] (**8**)

A solution of 3,6-dichloro-1,2-benzenedithiol (106 mg, 0.51 mmol, 1 eq.) and sodium methoxide (55 mg, 1.00 mmol, 2 eq.) in dried THF (15 mL) was stirred under nitrogen for one hour, a yellow colour appeared after 10 min. The [(pentamethylcyclopentadieneIr)$_2$(μ-Cl)$_2$] dimer (198 mg, 0.25 mmol, 0.5 eq.) was then added, the solution became dark red and was stirred for 15 min. The solvent was removed and the remaining solid was purified by chromatographic column (hexane/CH_2Cl_2 2:1). A red powder was obtained (240 mg, 89%).

Only the mononuclear complex exists in solution, as confirmed by ^{1}H NMR.

^{1}H NMR (400 MHz, $CDCl_3$): 7.31 (s, 2H, $H_{arom\ benzene}$), 2.16 (s, 15H, CH_3C_{arom}). ^{13}C NMR (100 MHz, $CDCl_3$): 153.2, 131.8, 124.0, 93.2, 10.7. MS (AP^+): 537.1 $[M+H]^+$. UV-vis (CH_2Cl_2, 1.0×10^{-4} M): λ_{max} 260 ($\varepsilon = 2.09 \times 10^4$ M^{-1}/cm), 305 ($\varepsilon = 0.94 \times 10^4$ M^{-1}/cm), 405 ($\varepsilon = 0.90 \times 10^4$ M^{-1}/cm), 536 ($\varepsilon = 0.10 \times 10^4$ M^{-1}/cm).

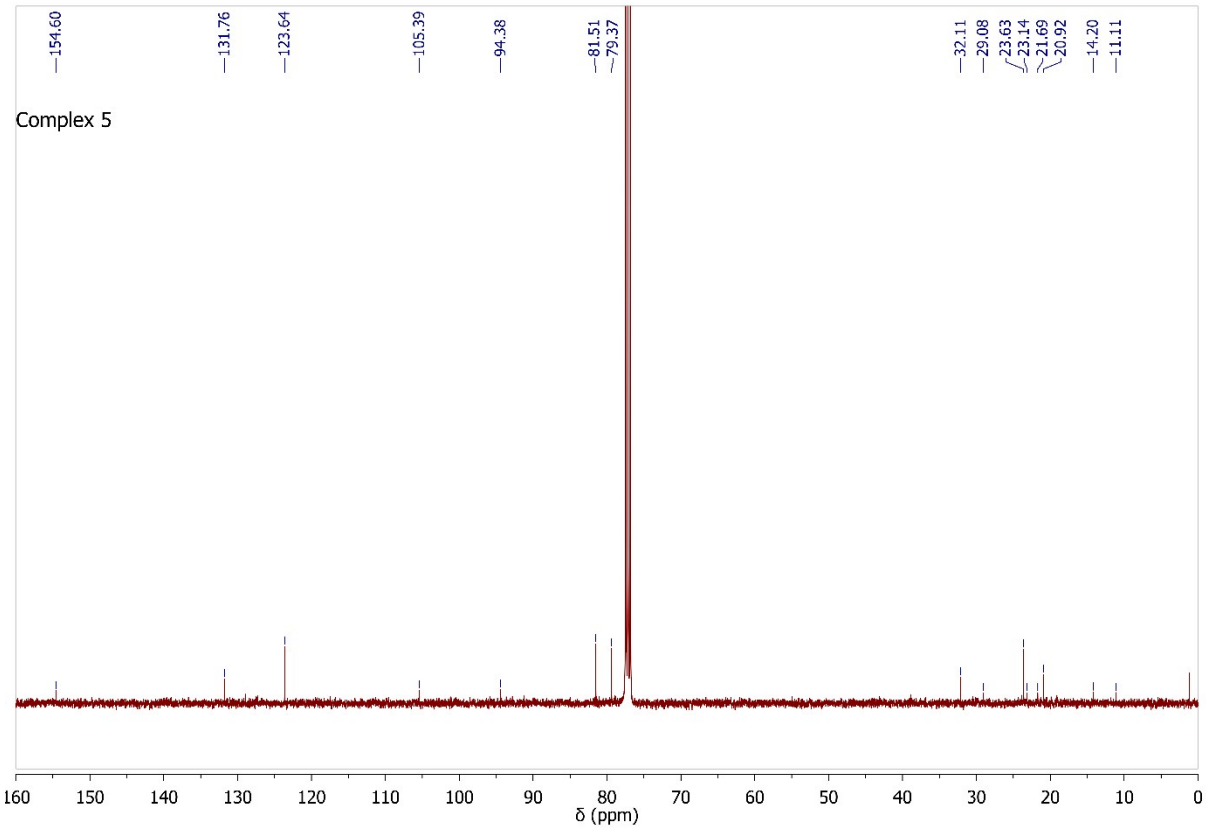

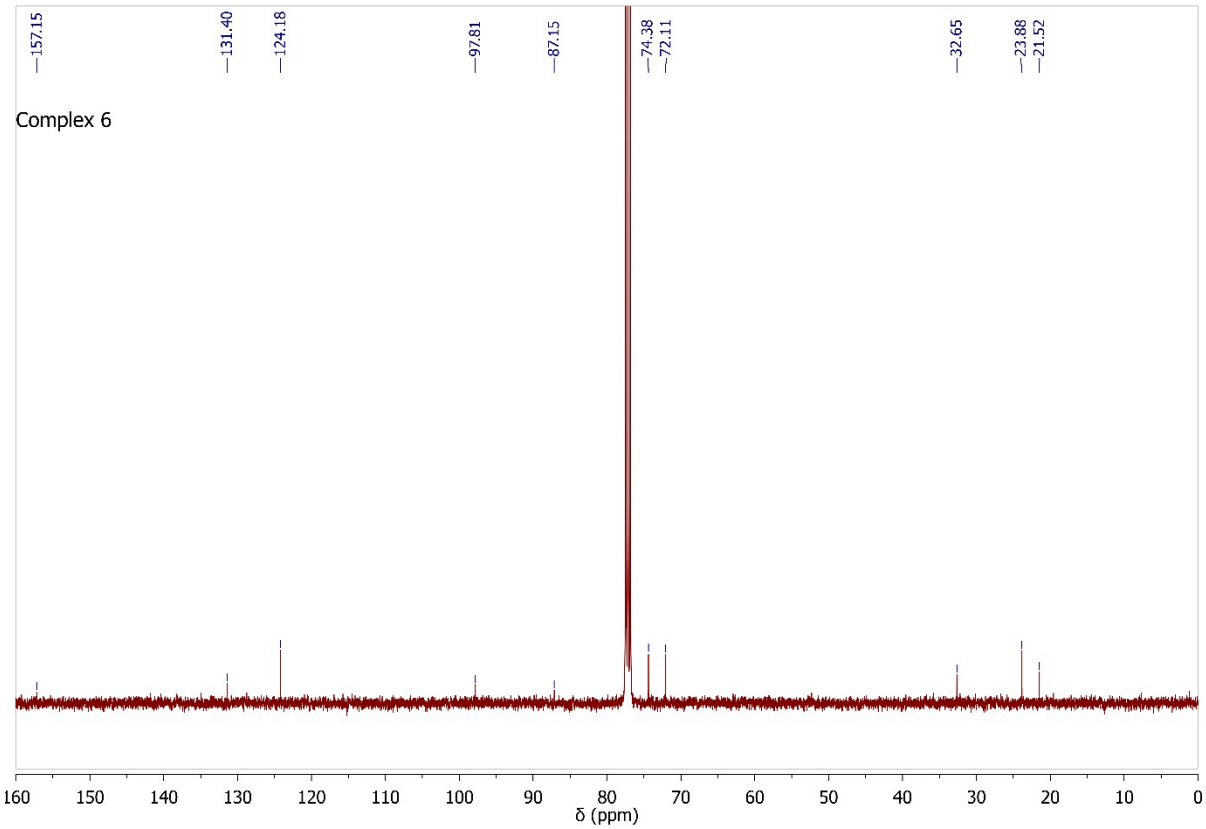

Figure S6a. ^{13}C NMR spectra of complexes **5** and **6** ($CDCl_3$, 100 MHz, 298 K).

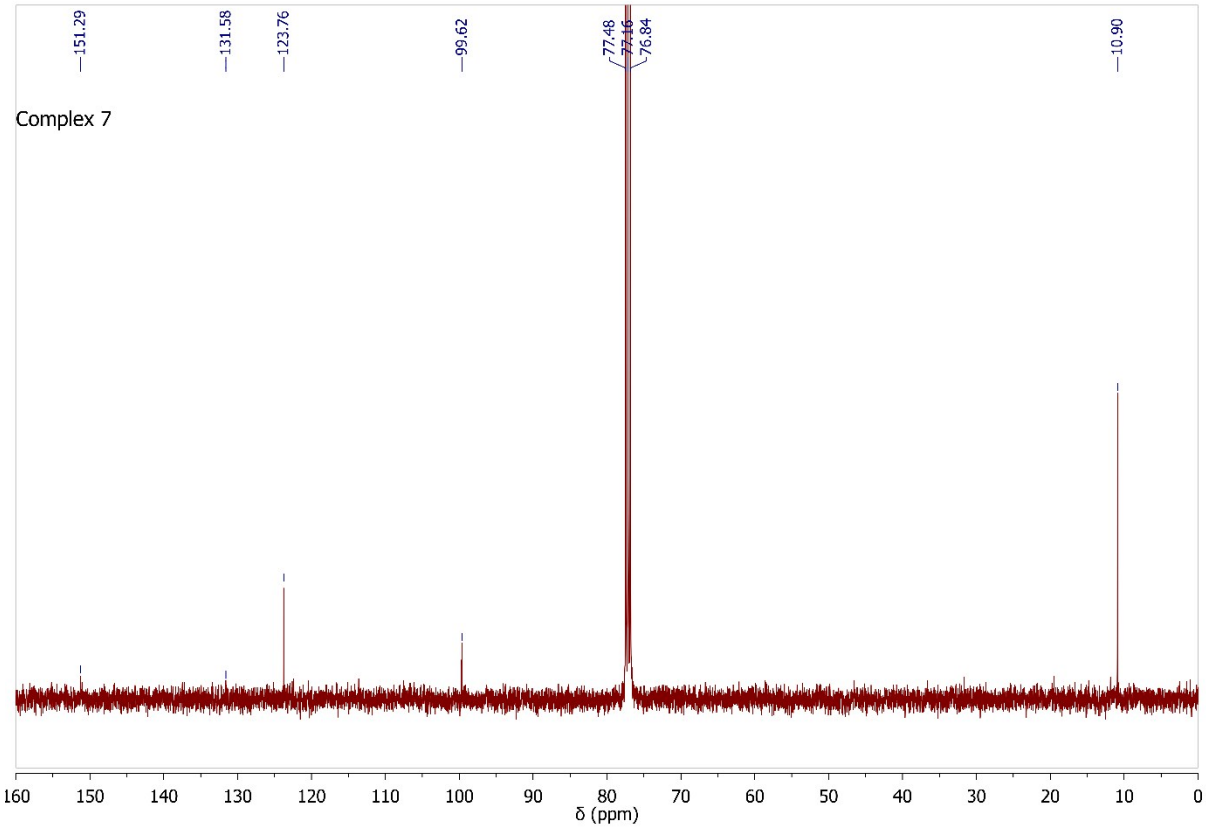

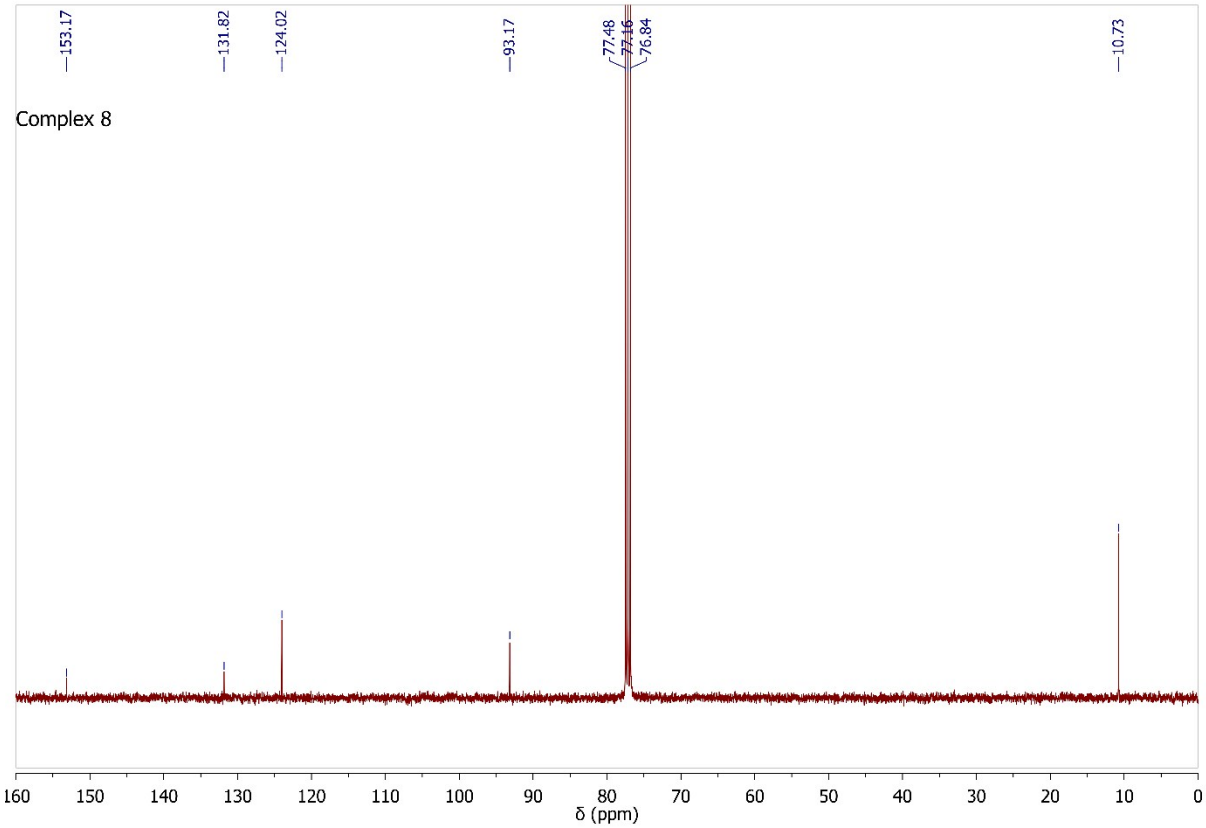

Figure S6b. ^{13}C NMR spectra of complexes **7** and **8** ($CDCl_3$, 100 MHz, 298 K).

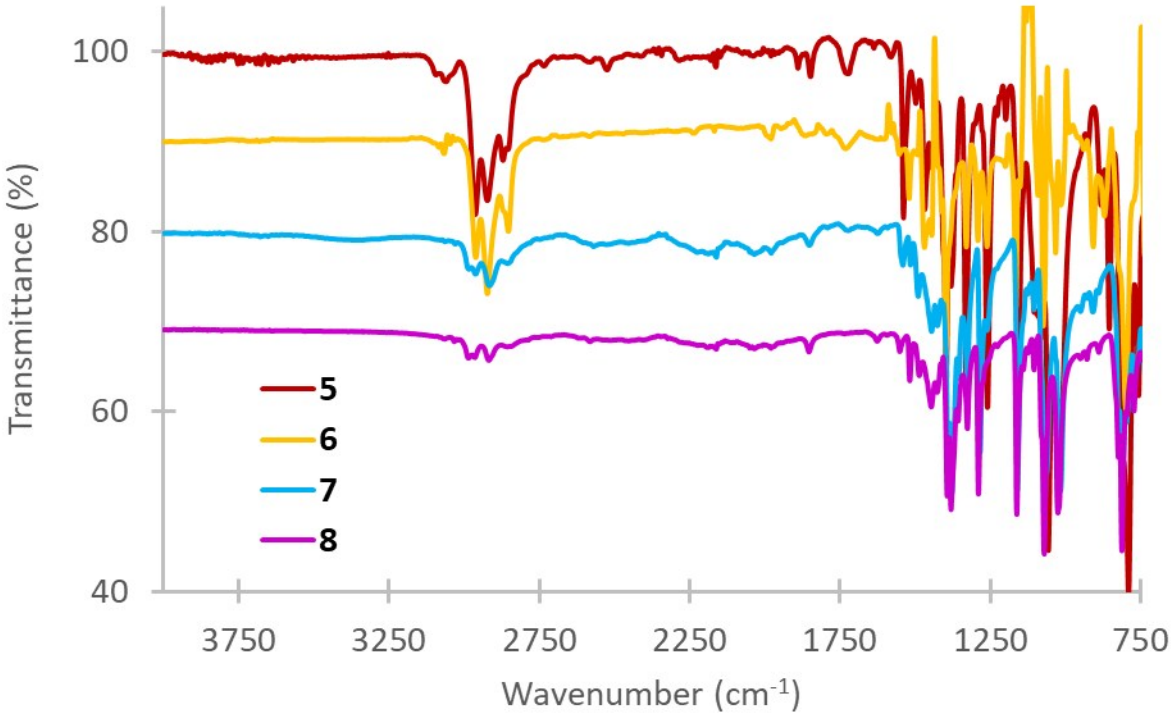

Figure S7. Infra-red spectra of complexes **5 – 8**, recorded as powders (spectra have been shifted along the y axis for clarity).

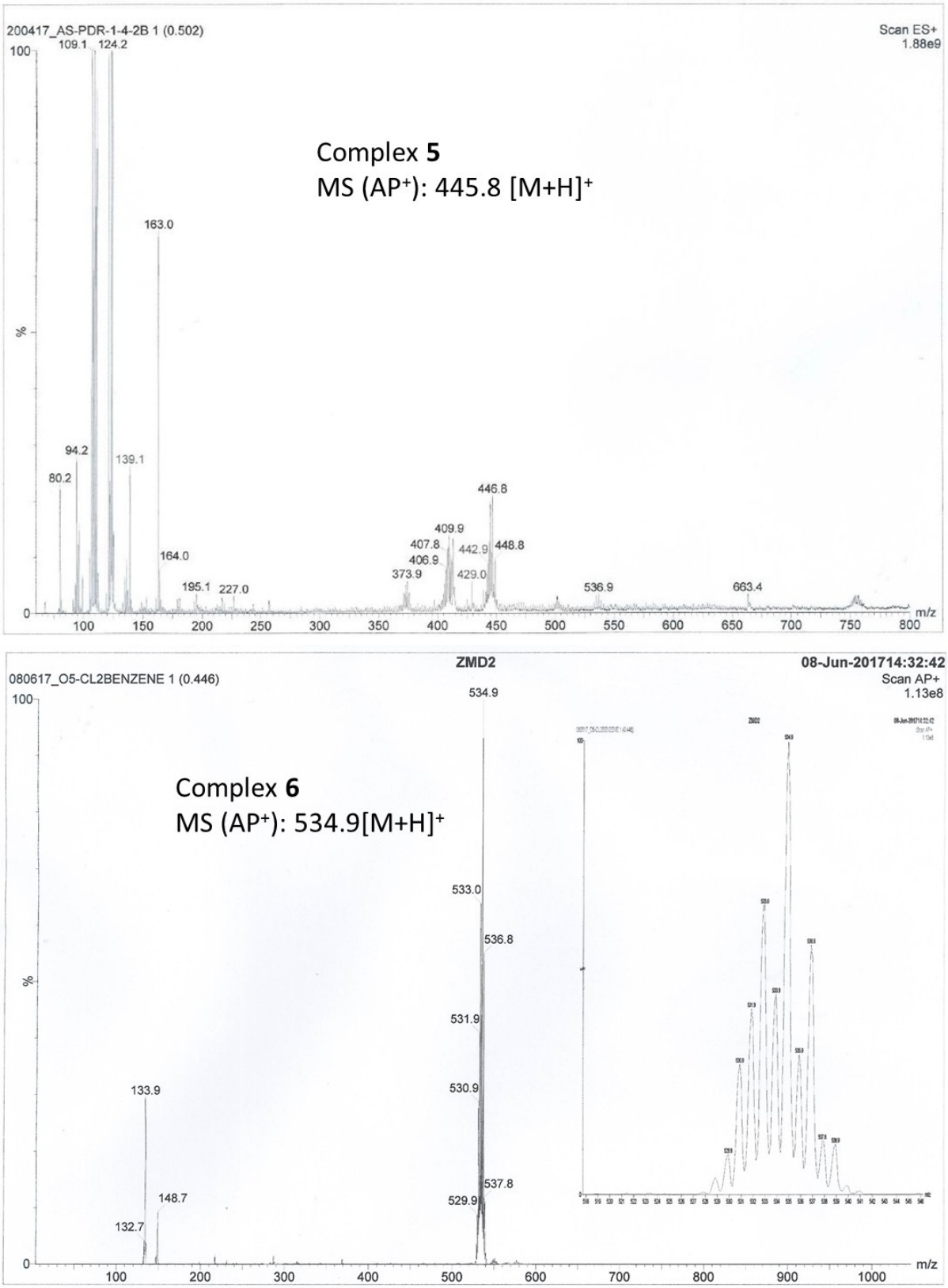

Figure S8a. Mass spectra of complexes **5** and **6** in methanol solutions, recorded in ESI+ mode.

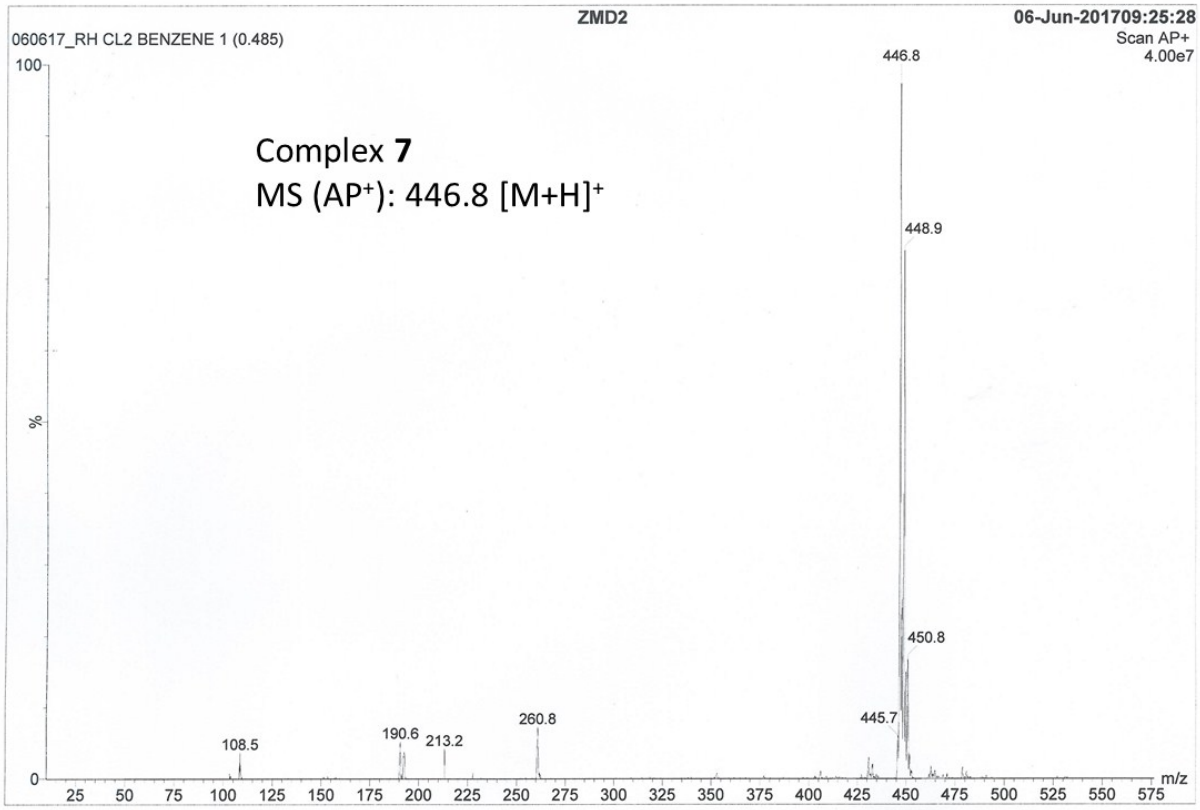

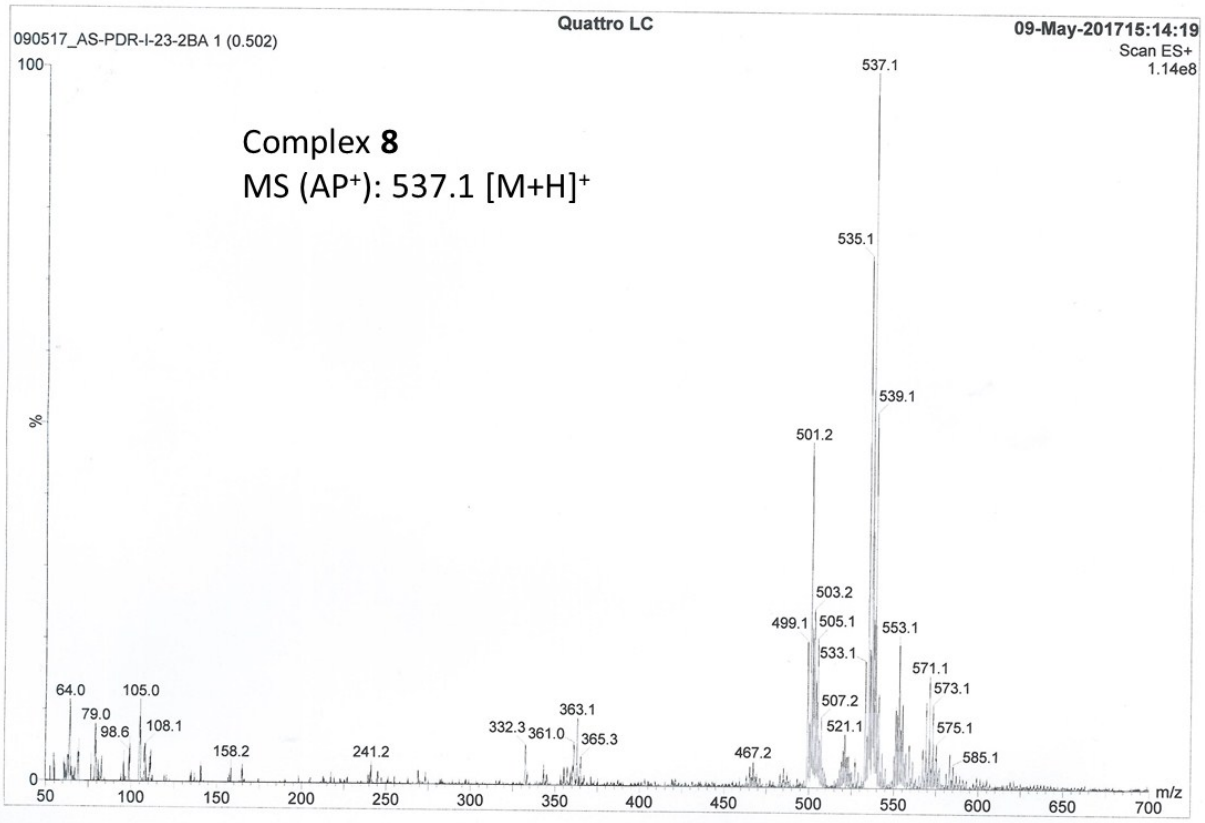

Figure S8b. Mass spectra of complexes **7** and **8** in methanol solutions, recorded in ESI+ mode.

5. Titration of complexes 5-8

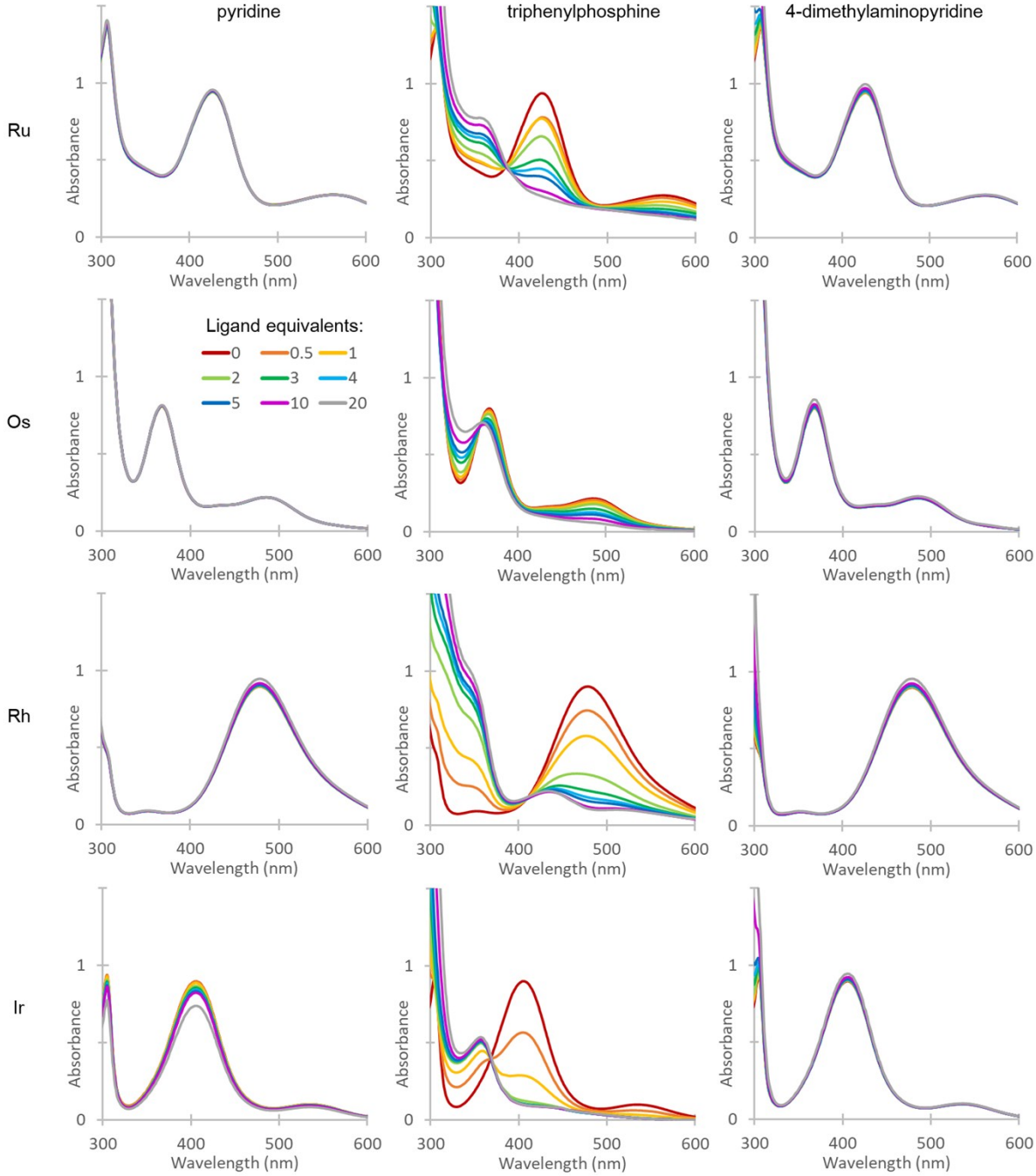

Figure S9. UV-Vis spectra of the titration of complexes **5 – 8** by DMAP, triphenylphosphine, and pyridine in CH_2Cl_2 (10^{-4} M, 298 K).

6. Crystallographic data

Table S1**.** X-ray crystallographic data for complexes **1**, **3**, **6**, and **8**, with s.u.s shown in parenthesis.

Complex	1	3	6	8
Formula	$C_{32}H_{36}Ru_2S_4$	$C_{32}H_{38}Rh_2S_4$	$C_{16}H_{16}Cl_2OsS_2$	$C_{16}H_{17}Cl_2IrS_2$
Formula weight	750.99	756.68	533.51	536.51
Crystal system	Monoclinic	Triclinic	Orthorhombic	Orthorhombic
Space group	$P2_1/n$	P-1	*Pbca*	*Pbca*
a (Å)	8.3501(3)	8.0369(3)	13.0325(9)	8.4853(7)
b (Å)	11.5760(4)	10.5256(3)	15.8037(10)	13.8473(13)
c (Å)	15.4298(5)	10.8572(4)	16.5142310)	29.535(2)
α (°)	90	61.5440(10)	90	90
β (°)	93.101(2)	69.2960(10)	90	90
γ (°)	90	79.238(2)	90	90
V (Å^3)	1489.27(9)	755.15(5)	3400.9(4)	3470.3(5)
Z	2	1	8	8
Density (Mg m^{-3})	1.675	1.664	2.084	2.054
Crystal size	0.72×0.15×0.12	0.66×0.36×0.19	0.39×0.34×0.21	1.07 × 0.07 × 0.07
Absorp coeff (mm^{-1})	10.983	11.571	19.258	12.949
Radiation type	Cu *K*α	Cu *K*α	Cu *K*α	Cu *K*α
T (K)	170.02	170.0	170.0	170.01
Reflections collected	10648	10493	33857	22761
Independent reflections	2530	2562	2874	2843
R_1	0.0702	0.0321	0.0379	0.0542
wR_2	0.1845	0.0814	0.0986	0.1439
Goodness of Fit	1.053	1.104	1.208	1.070

Table S2**.** Selected bond lengths (Å) for complexes **1**, **3**, **6**, and **8**.

Complex	1 (M = Ru)	3 (M = Rh)	6 (M = Os)	8 (M = Ir)
M1-M1'	3.6219(5)	3.5189(4)	-	-
M1-S1	2.3775(13)	2.3589(8)	2.2582(14)	2.249(3)
M1-S1'	2.4096(13)	-	-	-
M1-S2	2.3774(14)	2.3523(8)	2.2568(14)	2.246(3)
M1-S2'	-	2.3981(8)	-	-
M1- Cg	1.709	1.831	1.690	1.818

Table S3**.** Selected bond angles (°) for complexes **1**, **3**, **6**, and **8**.

Complex	1 (M = Ru)	3 (M = Rh)	6 (M = Os)	8 (M = ir)
S1-M1-S1'	81.68(5)	-	-	-
S1-M1-S2	84.54(5)	85.05(3)	87.68(5)	88.35(11)
S1-M1-S2'	-	84.69(3)	-	-
S2-M1-S1'	84.31(5)	-	-	-
S2-M1-S2'	-	84.42(3)	-	-
S1-M1- Cg	131.31	124.63	135.89	137.34
S2-M1- Cg	115.03	127.39	136.41	134.31
S1'-M1-Cg	131.31	-	-	-
S2'-M1-Cg	-	134.45	-	-

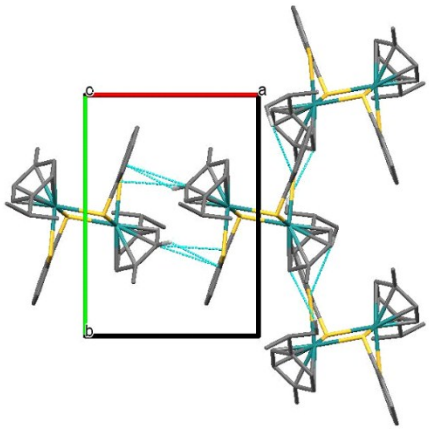

Compound **1** along the *c* axis

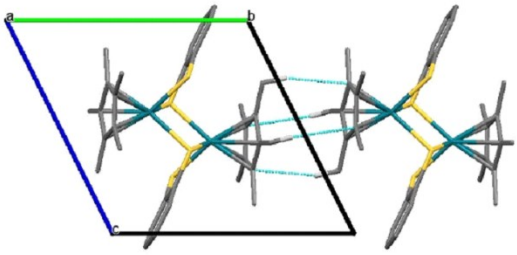

Compound **3** along the *a* axis

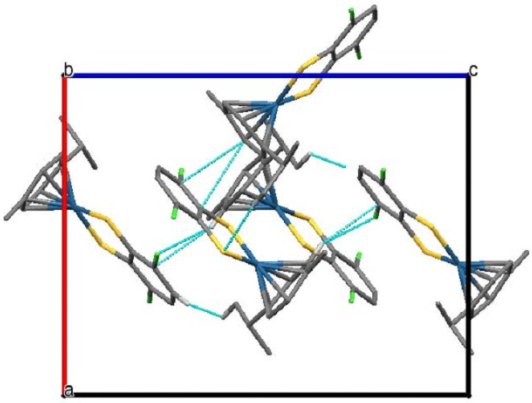

Compound **6** along the *b* axis

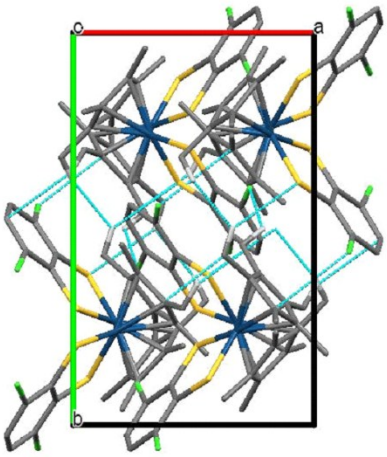

Compound **8** along the *c* axis

Figure S10. Packing diagram showing the short contacts of complex **1**, **3**, **6** and **8**.

7. Calculations data

Table S4**.** Distance table for the optimized structure of complex **1** (M11L/def2tzvp).

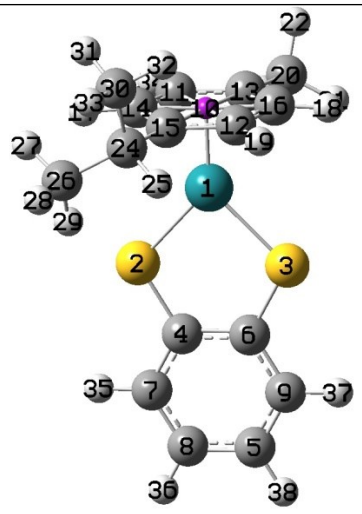

S1 (Ru)

		1	2	3	4	5
1	Ru	0.000000				
2	S	2.244215	0.000000			
3	S	2.242011	3.085469	0.000000		
4	C	3.197893	1.715057	2.691620	0.000000	
5	C	5.554672	4.481180	3.974675	2.766195	0.000000
6	C	3.196166	2.689941	1.715187	1.393200	2.391502
7	C	4.547374	2.708206	3.982849	1.391349	2.387840
8	C	5.556072	3.975823	4.481900	2.391860	1.387692
9	C	4.544514	3.981035	2.706525	2.404851	1.366648
Centroid		1.680925	3.653704	3.648512	4.852550	7.224816
11	C	2.171388	3.544157	4.205671	4.905820	7.408258
12	C	2.176878	4.228878	3.560932	5.169107	7.288404
13	C	2.180238	4.104315	3.651142	5.089935	7.259789
14	C	2.212860	3.358857	4.448687	4.894077	7.527639
15	C	2.184884	3.681550	4.122542	4.972716	7.414659
16	C	2.212243	4.448639	3.347191	5.265755	7.256492
		6	7	8	9	10
6	C	0.000000				
7	C	2.405524	0.000000			
8	C	2.766782	1.366722	0.000000		
9	C	1.390791	2.763320	2.388125	0.000000	
Centroid		4.849889	6.170565	7.226969	6.166032	0.000000
11	C	5.136405	6.111460	7.250612	6.476820	1.389900
12	C	4.934788	6.515464	7.449447	6.143256	1.389397
13	C	4.931831	6.406524	7.367255	6.157054	1.424253
14	C	5.271035	6.057398	7.270192	6.654751	1.396391
15	C	5.124654	6.206333	7.312053	6.445434	1.424048
16	C	4.883002	6.649713	7.518616	6.042449	1.396383
		11	12	13	14	15
11	C	0.000000				
12	C	2.779240	0.000000			
13	C	1.414398	2.432211	0.000000		
14	C	1.396121	2.411409	2.448483	0.000000	
15	C	2.432520	1.414952	2.847797	1.401519	0.000000
16	C	2.412132	1.394341	1.402959	2.791862	2.447948

Table S5**.** Distance table for the optimized structure of complex **2** (M11L/def2tzvp).

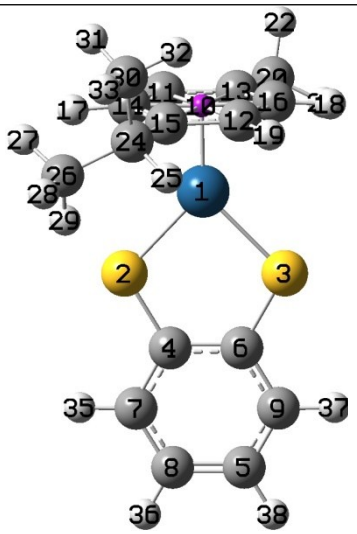

S2 (Os)

		1	2	3	4	5
1	Os	0.000000				
2	S	2.259972	0.000000			
3	S	2.258426	3.105068	0.000000		
4	C	3.210772	1.721182	2.699080	0.000000	
5	C	5.567837	4.485702	3.977666	2.764536	0.000000
6	C	3.208909	2.696557	1.721647	1.389654	2.391472
7	C	4.557356	2.707088	3.987784	1.389103	2.386307
8	C	5.569277	3.978494	4.487102	2.391663	1.385723
9	C	4.554500	3.985166	2.705567	2.400251	1.368149
Centroid		1.704820	3.690158	3.687059	4.889173	7.262124
11	C	2.185750	3.584766	4.228318	4.941097	7.438121
12	C	2.191125	4.248308	3.602004	5.192826	7.319518
13	C	2.194689	4.148010	3.670586	5.127358	7.292632
14	C	2.243570	3.403885	4.496151	4.941370	7.574422
15	C	2.198350	3.694426	4.163863	4.994304	7.443548
16	C	2.243986	4.496914	3.397881	5.315330	7.309416
		6	7	8	9	10
6	C	0.000000				
7	C	2.401175	0.000000			
8	C	2.765476	1.368165	0.000000		
9	C	1.388621	2.759313	2.386738	0.000000	
Centroid		4.886938	6.203871	7.263928	6.200239	0.000000
11	C	5.163380	6.146403	7.285539	6.499816	1.391526
12	C	4.967478	6.534128	7.474903	6.175406	1.390959
13	C	4.961458	6.444533	7.405599	6.182221	1.424934
14	C	5.316610	6.101035	7.317065	6.697951	1.401208
15	C	5.155007	6.221724	7.334672	6.475631	1.424739
16	C	4.935463	6.696942	7.570565	6.092369	1.401320
		11	12	13	14	15
11	C	0.000000				
12	C	2.782313	0.000000			
13	C	1.420386	2.431194	0.000000		
14	C	1.397872	2.418064	2.455029	0.000000	
15	C	2.431508	1.420694	2.848918	1.402034	0.000000
16	C	2.418967	1.396380	1.403332	2.800865	2.454643

Table S6**.** Distance table for the optimized structure of complex **3** (M11L/def2tzvp).

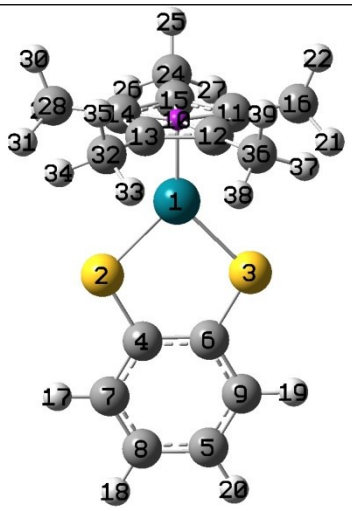

S3 (Rh)

		1	2	3	4	5
1	Rh	0.000000				
2	S	2.237168	0.000000			
3	S	2.237481	3.091437	0.000000		
4	C	3.179899	1.709736	2.690651	0.000000	
5	C	5.538947	4.478627	3.969718	2.768931	0.000000
6	C	3.179745	2.690937	1.709093	1.396850	2.393124
7	C	4.530196	2.702518	3.979463	1.391170	2.387474
8	C	5.539143	3.970863	4.477811	2.393321	1.388105
9	C	4.529796	3.979913	2.701343	2.406891	1.366098
Centroid		1.811674	3.762125	3.760780	4.963603	7.339611
11	C	2.187320	4.390072	3.473062	5.272588	7.335751
12	C	2.173410	4.211131	3.667573	5.200233	7.372306
13	C	2.175025	3.649610	4.230719	5.006687	7.508914
14	C	2.186021	3.482746	4.381807	4.957297	7.551721
15	C	2.167747	3.951978	3.925639	5.099815	7.421498
		6	7	8	9	10
6	C	0.000000				
7	C	2.406768	0.000000			
8	C	2.768753	1.366200	0.000000		
9	C	1.391066	2.761657	2.387392	0.000000	
Centroid		4.962836	6.280474	7.340257	6.279055	0.000000
11	C	4.953696	6.648954	7.553559	6.144743	1.213057
12	C	5.010414	6.541647	7.501842	6.241811	1.206911
13	C	5.208928	6.234573	7.370988	6.553885	1.207399
14	C	5.269407	6.150988	7.338871	6.643919	1.212798
15	C	5.090329	6.389141	7.428196	6.373785	1.203771
		11	12	13	14	15
11	C	0.000000				
12	C	1.410833	0.000000			
13	C	2.303188	1.433777	0.000000		
14	C	2.310583	2.302190	1.410174	0.000000	
15	C	1.424604	2.289730	2.290416	1.425763	0.000000

Table S7**.** Distance table for the optimized structure of complex **4** (M11L/def2tzvp).

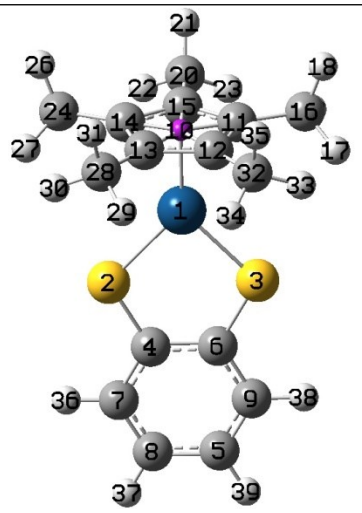

S4 (Ir)

		1	2	3	4	5
1	Ir	0.000000				
2	S	2.248783	0.000000			
3	S	2.249154	3.096187	0.000000		
4	C	3.195226	1.714060	2.692144	0.000000	
5	C	5.553859	4.480732	3.971525	2.766694	0.000000
6	C	3.194991	2.692512	1.713197	1.392715	2.392132
7	C	4.542905	2.702761	3.980138	1.389440	2.386528
8	C	5.554090	3.972920	4.479716	2.392307	1.386820
9	C	4.542419	3.980712	2.701325	2.402774	1.367012
Centroid		1.832303	3.794914	3.792808	4.999908	7.375043
11	C	2.211666	4.426714	3.512769	5.314218	7.378683
12	C	2.187219	4.234458	3.694961	5.226981	7.398881
13	C	2.189721	3.675194	4.257969	5.036052	7.536968
14	C	2.209663	3.524704	4.416470	5.001928	7.594218
15	C	2.182974	3.985156	3.953595	5.136516	7.457999
		6	7	8	9	10
6	C	0.000000				
7	C	2.402676	0.000000			
8	C	2.766536	1.367126	0.000000		
9	C	1.389351	2.759120	2.386429	0.000000	
Centroid		4.998767	6.313985	7.375930	6.312008	0.000000
11	C	4.997339	6.688518	7.596082	6.185501	1.216227
12	C	5.038922	6.565283	7.527767	6.267097	1.208838
13	C	5.237861	6.260396	7.398833	6.580150	1.209535
14	C	5.310494	6.193314	7.382776	6.682706	1.215813
15	C	5.125371	6.424551	7.465767	6.406653	1.204088
		11	12	13	14	15
11	C	0.000000				
12	C	1.412908	0.000000			
13	C	2.308612	1.438123	0.000000		
14	C	2.316496	2.307154	1.411931	0.000000	
15	C	1.426689	2.291397	2.292358	1.428220	0.000000

Table S8**.** Molecular orbitals involved in the five main calculated singlet electronic transitions of the UV-visible spectrum of complex **1** and their relative weights determined by TD-DFT calculations. The molecular orbitals are shown in Figure 8.

Main MOs	Relative weights
80 → 82	0.49307
77 → 86	0.41551
78 → 89	0.48475
78 → 82	0.52760
81 → 91	0.51067

Table S9**.** Molecular orbitals, with ranking order and energy (in a.u.) for compound **1.**

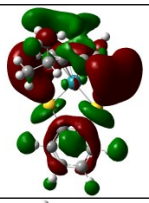	92 -0.00044	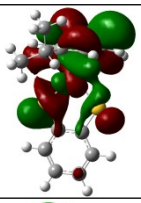	85 -0.05405	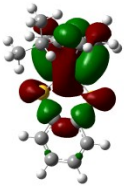	78 -0.21750
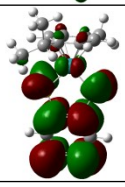	91 -0.02027	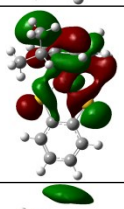	84 -0.05485	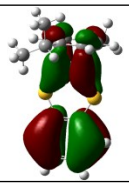	77 -0.21750
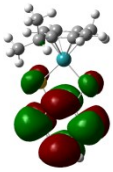	90 -0.02725	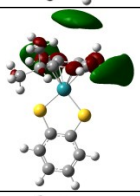	83 -0.06794	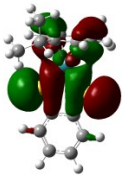	76 -0.24320
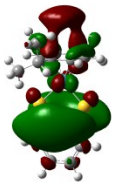	89 -0.02935	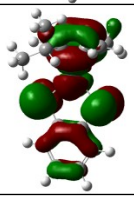	82 LUMO -0.10876	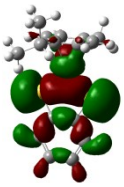	75 -0.26989
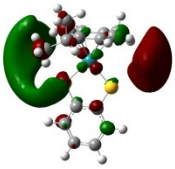	88 -0.04528	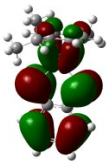	81 HOMO -0.18211		74 -0.27103
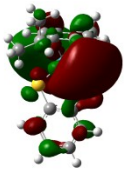	87 -0.04809	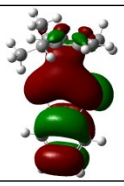	80 HOMO-1 -0.19444	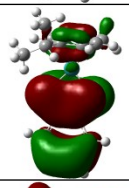	73 -0.27518
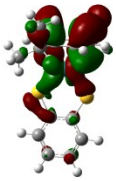	86 -0.04809	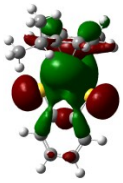	79 -0.19757	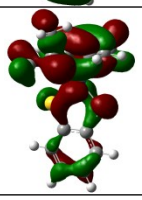	72 -0.30119

Table S10**.** Thermochemistry of the reactions between complexes **1** – **4**, pyridine, DMAP, and triphenylphosphine, with computed zero point corrected Gibbs free energies of all the species**.**

	E + thermal corr.	ZPE	E + thermal corr. + ZPE	Binding Energy (kcal/mol)	Binding Energy (with ZPE) (kcal/mol)
DMAP	-303.614389	0.104855	-303.509534		
PPh_3	-1036.180024	0.269664	-1035.910360		
Pyridine	-248.257266	0.087290	-248.169976		
1	-1511.943676	0.293928	-1511.649748		
2	-1507.729921	0.293636	-1507.436285		
3	-1528.232712	0.302289	-1527.930423		
4	-1522.019875	0.302137	-1521.717738		
1 + DMAP	-1815.543915	0.400665	-1815.143250	8.9	10.1
1 + PPh_3	-2548.114716	0.565175	-2547.549541	5.6	6.6
1 + Pyridine	-1760.183901	0.383337	-1759.800564	10.7	12.0
2 + DMAP	-1811.327836	0.400587	-1810.927249	10.3	11.7
2 + PPh_3	-2543.896037	0.566304	-2543.329733	8.7	10.6
2 + Pyridine	-1755.968288	0.383172	-1755.585116	11.9	13.3
3 + DMAP	-1831.830169	0.408798	-1831.421371	10.6	11.7
3 + PPh_3	-2564.407653	0.574194	-2563.833459	3.2	4.6
3 + Pyridine	-1776.471371	0.391595	-1776.079776	11.7	12.9
4 + DMAP	-1825.614306	0.409080	-1825.205226	12.5	13.8
4 + PPh_3	-2558.193066	0.574630	-2557.618436	4.3	6.1
4 + Pyridine	-1770.254293	0.391674	-1769.862619	14.3	15.7

8. ^{1}H DOSY NMR

Diffusion ordered spectroscopy experiments were carried out on complex **1** in $CDCl_3$ (10 mM). This was done to establish the difference between single and monomeric and dimeric metal species in the same sample. Samples were run at varying temperatures as shown in Fig. S11.

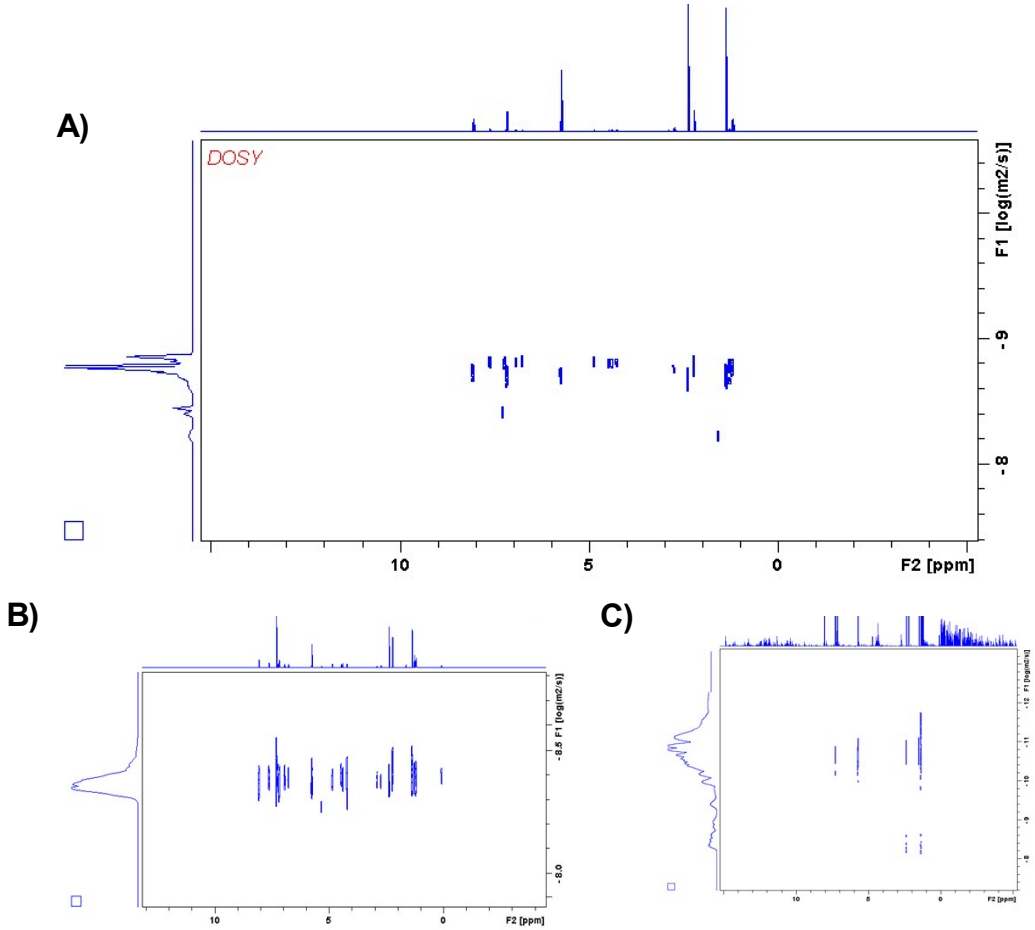

Figure S11. Snapshot of raw ^{1}H DOSY data from complex **1** processed using Bruker Topspin software carried out at 298 (A), 278 (B) and 328 (C) K.

From the room temperature data (298 K) a horizontal slice of the ^{1}H proton peak from both the monomer ($D = 1.52 \times 10^{-9}$ m^2 S^{-1}) and dimer ($D = 1.75 \times 10^{-9}$ m^2 S^{-1}) was taken so that the monomer and dimer proton signals could be isolated. This is shown in Fig S.12.

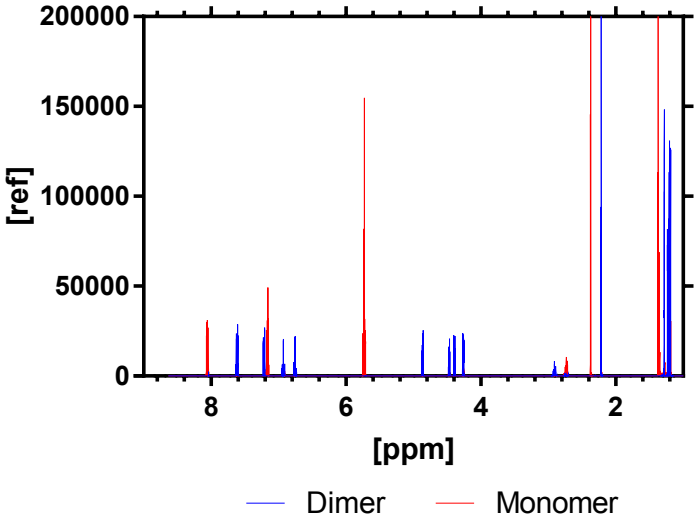

Figure S12. Isolated ^{1}H proton signal from dimer (blue) and monomer (red) signals

The signals at 5.7 and 4.8 ppm were then extracted to determine the exact diffusion of the samples at different temperatures, and the ratio of the two proton sources compared to give the ratio of monomer (*M*) : Dimer (*D*) present at that temperature. This data is shown in Table S11 with raw data show nin Fig. S14. This data indicates that as the temperature was increased the concentration of dimer was reduced significantly, so that at 318 K there was insufficient concentration of dimer to determine an accurate diffusion value and the accuracy of the fits was greatly reduced. Within the sample the diffusion of the solvent peaks ($CDCl_3$) decreased as the temperature was raised however this is likely due to the changing concentration of monomer / dimer complexes present within the sample affecting solvent viscosity.

Table S11. ^{1}H DOSY NMR of complex **1** at different temperatures.

Temperature / K	*$CDCl_3$ D* / x10^{9} M^{2} S^{-1}	*M* Diffusion / x10^{9} M^{2} S^{-1}	*D* Diffusion / x10^{9} M^{2} S^{-1}	Ratio of peaks (^{1}H *M* / ^{1}H *D*)
278 K	4.57 ± 0.10	4.52 ± 0.10	4.60 ± 0.10	1.32
298 K	3.63 ± 0.10	1.52 ± 0.10	1.75 ± 0.10	2.70
328 K	3.89 ± 0.10	0.02 ± 0.10	- (too small)*	30.48

9. References

1. Tönnemann, J.; Risse, J.; Grote, Z.; Scopelliti, R.; Severin, K., Efficient and Rapid Synthesis of Chlorido-Bridged Half-Sandwich Complexes of Ruthenium, Rhodium, and Iridium by Microwave Heating. *Eur. J. Inorg. Chem.* **2013,** *2013* (26), 4558-4562.
2. Xi, R.; Abe, M.; Suzuki, T.; Nishioka, T.; Isobe, K., Synthesis and characterization of pentamethylcyclopentadienylrhodium(III) and -iridium(III) complexes with 1,2-benzenedithiolate · [(Cp∗Rh)2(μ(S)-1,2-C6H4S2-S,S′)2], [(Cp∗Rh)2(μ(S)-1,2-C6H4S2-S,S′)(μ(S)-1,2-C6H4S(SO2)-S,S′)] and [(Cp∗Ir)(1,2-C6H4S2-S,S′)] (Cp∗ = η5-C5(CH3)5) Professor Peter M. Maitlis on the occasion of his 65th birthday and in recognition of his pioneer contributions to this field. *J. Organomet. Chem.* **1997,** *549* (1–2), 117-125.
3. Fulmer, G. R.; Miller, A. J. M.; Sherden, N. H.; Gottlieb, H. E.; Nudelman, A.; Stoltz, B. M.; Bercaw, J. E.; Goldberg, K. I., NMR Chemical Shifts of Trace Impurities: Common Laboratory

Solvents, Organics, and Gases in Deuterated Solvents Relevant to the Organometallic Chemist. *Organometallics* **2010,** *29* (9), 2176-2179.
4. Swift, T.; Hoskins, R.; Telford, R.; Plenderleith, R.; Pownall, D.; Rimmer, S., Analysis using size exclusion chromatography of poly(N-isopropyl acrylamide) using methanol as an eluent. *J. Chromatogr. A* **2017,** *1508*, 16-23.
5. Cosier, J.; Glazer, A. M., A nitrogen-gas-stream cryostat for general X-ray diffraction studies. *J. Appl. Crystallogr.* **1986,** *19* (2), 105-107.
6. Bruker-AXS, APEX2. Version 2014.11-0. *Madison* **2014,** *Wisconsin*, USA.
7. Dolomanov, O. V.; Bourhis, L. J.; Gildea, R. J.; Howard, J. A. K.; Puschmann, H., OLEX2: a complete structure solution, refinement and analysis program. *J. Appl. Crystallogr.* **2009,** *42* (2), 339-341.
8. Sheldrick, G. M., XS. Version 2013/1. *Georg-August-Universität Göttingen* **2013,** *Göttingen*, Germany.
9. Sheldrick, G., SHELXT - Integrated space-group and crystal-structure determination. *Acta Crystallographica Section A* **2015,** *71* (1), 3-8.
10. Macrae, C. F.; Bruno, I. J.; Chisholm, J. A.; Edgington, P. R.; McCabe, P.; Pidcock, E.; Rodriguez-Monge, L.; Taylor, R.; van de Streek, J.; Wood, P. A., Mercury CSD 2.0 - new features for the visualization and investigation of crystal structures. *J. Appl. Crystallogr.* **2008,** *41* (2), 466-470.
11. Peverati, R.; Truhlar, D. G., M11-L: A Local Density Functional That Provides Improved Accuracy for Electronic Structure Calculations in Chemistry and Physics. *The Journal of Physical Chemistry Letters* **2012,** *3* (1), 117-124.
12. Nicklass, A.; Dolg, M.; Stoll, H.; Preuss, H., Ab initio energy-adjusted pseudopotentials for the noble gases Ne through Xe: Calculation of atomic dipole and quadrupole polarizabilities. *J. Chem. Phys.* **1995,** *102* (22), 8942-8952.
13. Weigend, F.; Ahlrichs, R., Balanced basis sets of split valence, triple zeta valence and quadruple zeta valence quality for H to Rn: Design and assessment of accuracy. *Phys. Chem. Chem. Phys.* **2005,** *7* (18), 3297-3305.
14. Cossi, M.; Rega, N.; Scalmani, G.; Barone, V., Energies, structures, and electronic properties of molecules in solution with the C-PCM solvation model. *J. Comput. Chem.* **2003,** *24* (6), 669-681.
15. M. J. Frisch, G. W. T., H. B. Schlegel, G. E. Scuseria, M. A. Robb, J. R. Cheeseman, G. Scalmani, V. Barone, G. A. Petersson, H. Nakatsuji, X. Li, M. Caricato, A. Marenich, J. Bloino, B. G. Janesko, R. Gomperts, B. Mennucci, H. P. Hratchian, J. V. Ortiz, A. F. Izmaylov, J. L. Sonnenberg, D. Williams-Young, F. Ding, F. Lipparini, F. Egidi, J. Goings, B. Peng, A. Petrone, T. Henderson, D. Ranasinghe, V. G. Zakrzewski, J. Gao, N. Rega, G. Zheng, W. Liang, M. Hada, M. Ehara, K. Toyota, R. Fukuda, J. Hasegawa, M. Ishida, T. Nakajima, Y. Honda, O. Kitao, H. Nakai, T. Vreven, K. Throssell, J. A. Montgomery, Jr., J. E. Peralta, F. Ogliaro, M. Bearpark, J. J. Heyd, E. Brothers, K. N. Kudin, V. N. Staroverov, T. Keith, R. Kobayashi, J. Normand, K. Raghavachari, A. Rendell, J. C. Burant, S. S. Iyengar, J. Tomasi, M. Cossi, J. M. Millam, M. Klene, C. Adamo, R. Cammi, J. W. Ochterski, R. L. Martin, K. Morokuma, O. Farkas, J. B. Foresman, and D. J. Fox *Gaussian 09, Revision E.01*, Gaussian, Inc.: Wallingford CT, 2016.
16. Mashima, K.; Kaneyoshi, H.; Kaneko, S.-i.; Mikami, A.; Tani, K.; Nakamura, A., Chemistry of Coordinatively Unsaturated Bis(thiolato)ruthenium(II) Complexes (η6-arene)Ru(SAr)2 [SAr = 2,6-Dimethylbenzenethiolate, 2,4,6-Triisopropylbenzenethiolate; (SAr)2 = 1,2-Benzenedithiolate; Arene = Benzene, p-Cymene, Hexamethylbenzene]. *Organometallics* **1997,** *16* (5), 1016-1025.
17. Cabeza, J. A.; Garcia-Granda, S.; Perez-Priede, M.; Van der Maelen, J. F., Bis([mu]-[eta]2-benzene-1,2-dithiolato-[kappa]3S,S':S')bis[([eta]6-p-cymene)ruthenium(II)]. *Acta Crystallographica Section E* **2002,** *58* (5), m189-m190.